Article:
Li, X, Gadzinsky, A, Gong, L et al. (9 more authors) (2018) Cbl Ubiquitin Ligases Control B Cell Exit from the Germinal-Center Reaction. Immunity, 48 (3). 530-541.e6. ISSN 1074-7613

https://doi.org/10.1016/j.immuni.2018.03.006

Cbl ubiquitin ligases control the exit checkpoint of the germinal center reaction

Xin Li[1,2], Adeline Gadzinsky[1], Haijun Tong[1,2], Liying Gong[1,3], Virginie Calderon[1], Yue Li[1,4], Daisuke Kitamura[5], Ulf Klein[6], Wallace Y. Langdon[7], Fajian Hou[8], and Yong-Rui Zou[9] & Hua Gu[1,2,3,10]

[1]Montreal Clinical Research Institute, Montreal, Quebec H2W 1R7, Canada
[2]Department of Microbiology and Immunology, University of Montreal, Montreal, Quebec H3T 1J4, Canada
[3]Division of Experimental Medicine, McGill University, Montreal, Quebec H3A 0G4, Canada
[4]Department of Microbiology and Immunology, McGill University, Montreal, Quebec H3A 0G4, Canada
[5]Research Institute for Biomedical Sciences, Tokyo University of Sciences, Noda, Chiba 162-8601, Japan
[6] Leeds Institute of Cancer and Pathology, School of Medicine, University of Leeds, Leeds LS97TF, United Kingdom
[7] School of Biomedical Sciences, University of Western Australia, Crawley, Western Australia 6009, Australia
[8]Shanghai Institute of Biochemistry and Cell Biology, Chinese Academy of Sciences, Shanghai 200031, China
[9]The Feinstein Institute for Medical Research, Manhasset, New York 11030, USA
[10]Lead Contact

Correspondence: hua.gu@ircm.qc.ca

Highlights

Antibody affinity maturation depends on B cell intrinsic Cbls

Cbls control the clonal expansion of high B cells in GCs

Cbls are dynamically regulated in GC DZ and LZ B cells and downregulated upon sensing strong CD40 and BCR signaling

Cbls prevent nuclear Irf4 accumulation by ubiquitinating Irf4

In Brief

How B cells are retained in the germinal centers (GC) for affinity driven selection remains unclear. Gu and colleagues demonstrate that CBL-Irf4 constitutes an ubiquitination-dependent regulatory cascade to control the clonal expansion of B cells in GCs until high affinity BCRs are acquired.

SUMMARY

Selective expansion of high affinity B cells in the germinal center (GC) is a key event of the antibody affinity maturation. It remains elusive how GC B cells with improved affinity decide to continue affinity-driven selection or differentiate into plasma cells (PCs) or memory B cells. Here we found that ablation of E3 ubiquitin ligases Cbl and Cbl-b (Cbls) impaired clonal expansion of high affinity GC B cells due to the earlier exit from the GC cycle. Cbls were highly expressed in GC light zone (LZ) as compared to dark zone (DZ) B cells and impeded PC differentiation by promoting Irf4 ubiquitination. CD40 and BCR stimulation reduced Cbl proteins and concomitantly increased Irf4 expression. Increased Irf4 expression alone was sufficient to abolish GC affinity selection. Thus, by promoting Irf4 ubiquitination Cbls control a GC program that prevents high affinity B cells from prematurely exiting the GC cycle to ensure affinity-driven clonal expansion.

Key words:
Germinal center, B cell, Cbl ubiquitin ligase, antibody affinity maturation, Irf4.

INTRODUCTION

Production of high affinity antibodies is central to T cell-dependent humoral immunity against pathogens and occurs in germinal centers (GC) through a process termed antibody affinity maturation (Liu et al., 1989; Rajewsky, 1996). Upon encounter with antigen, activated B cells enter GCs to undergo clonal expansion and somatically mutate their B-cell antigen receptor (BCR) genes via activation-induced cytidine deaminase (AID)-mediated somatic hypermutation (SHM) in the anatomically distinct dark zone (DZ) (Allen et al., 2007; Berek et al., 1991; Jacob et al., 1991; Muramatsu et al., 2000; Victora and Nussenzweig, 2012). B cells with a mutant BCR then migrate to the light zone (LZ) to compete for the antigen presented by follicular dendritic cells (FDC) and the help from T follicular helper (Tfh) cells (Allen et al., 2007; Crotty, 2011; Ramiscal and Vinuesa, 2013; Shulman et al., 2014; Victora and Nussenzweig, 2012). Higher affinity BCRs have advantages to compete for the antigen, allowing B cells to receive more help such as CD40L stimulation from Tfh cells (Gitlin et al., 2014; Meyer-Hermann et al., 2012; Schwickert et al., 2007; Victora and Nussenzweig, 2012). Surviving GC B cells with improved affinity to the antigen may terminate the GC B cell fate and differentiate into memory B cells or plasma cells (PCs), or migrate back to the DZ for a further round of SHM and clonal expansion (Bannard and Cyster, 2017; De Silva and Klein, 2015; Dufaud et al., 2017; Mesin et al., 2016; Shlomchik and Weisel, 2012; Victora and Nussenzweig, 2012). The spatial and temporal circulation between the GC DZ and LZ enables B cells with higher affinity BCRs being preferentially expanded and selected to enter the memory or PC pool.

Given the critical role of such a GC inter-zonal circulation in the generation and selection of high affinity BCR-expressing B cells, much effort has been invested to understand the mechanisms by which B cells are instructed to stay in or exit the DZ-LZ cycle to become memory B cells or PCs. At the transcriptional level, maintenance

of the GC B cell fate is controlled by GC B cell promoting transcription factors such as Bcl6 (Basso and Dalla-Favera, 2012). In contrast, the identity of PCs depends on the transcription factors Blimp1 and Irf4 (Klein et al., 2006; Sciammas et al., 2006; Shapiro-Shelef et al., 2003). These two groups of transcription factors antagonistically regulate each other and dictate the steady-state distinctive characteristics of GC B cells and PCs, respectively (Nutt et al., 2015; Shapiro-Shelef and Calame, 2005). In addition to these transcription factors, Myc, Foxo1, and NFκB have been reported to provide additional layers of regulation during the GC reaction (Calado et al., 2012; De Silva and Klein, 2015; Dominguez-Sola et al., 2015; Dominguez-Sola et al., 2012; Heise et al., 2014; Inoue et al., 2017; Sander et al., 2015). Inactivation of NFκB, or Myc in GC B cells results in the collapse of the GCs, due to the impaired cycling of LZ B cells to the DZ. Foxo1 is essential for the DZ phenotype; mice with deletion of *Foxo1* in GC B cells have only LZ cells. However, the molecular mechanisms that sense BCR affinity cues in GC B cells and instructs B cells to continue the DZ and LZ cycle or to initiate the differentiation program to PCs are not fully defined.

Cbl and Cbl-b (Cbls) are members of the Cbl family of E3 ubiquitin ligases expressed in hematopoietic cells (Huang and Gu, 2008). In B cells, they play a crucial role in the induction of immune tolerance, possibly by regulating the negative selection of autoreactive B cells (Kitaura et al., 2007). Inactivation of Cbls using the *Cd19-cre* allele results in a moderate increase in IgM and reduction in IgG isotypes of T-cell dependent antibody responses (Kitaura et al., 2007). Here, we examined the function of Cbls in the GC reaction. We found that CBLs are essential for the selection of high affinity GC B cells and antibody affinity maturation. In GCs, the expression of Cbl proteins is minimal in DZ B cells and significantly increased in LZ B cells. They suppress Irf4 expression by promoting Irf4 ubiquitination. Ablation of Cbls in GC B cells increases the expression of Irf4, leading to impaired clonal expansion of high affinity B cells and expedited GC differentiation, despite normal SHM and DZ-LZ cycling of GC B cells. Consistent with this result, ectopic expression

of Irf4 alone or inactivation of the ubiquitin ligase activity of Cbls is sufficient to recapitulate the GC phenotypes found in Cbls mutant mice. Thus, our data indicate that B cell-intrinsic Cbls-Irf4 axis constitutes an ubiquitination dependent regulatory cascade that temporally controls GC B cells to stay in the DZ-LZ cycle until the acquisition of high affinity BCRs.

RESULTS

Expression patterns of Cbls in B cell subsets and the GC reaction

To evaluate whether Cbl proteins regulate T-dependent antibody response, we first examined the expression patterns of Cbl and Cbl-b in naïve and GC B cells. We found that decreased amounts of both *Cbl* and *Cbl-b* mRNA in GC B cells as compared to naïve B cells; however, GC B cells expressed higher amounts of Cbl and Cbl-b proteins as compared to naïve B cells (**Figures 1A, 1B** and **S1A**). The marked alteration seemed to be a GC phenomenon, since activation of B cells with anti-IgM or anti-CD40 induced only a mild increase or a decrease in both Cbl and Cbl-b proteins, respectively (**Figure S1B**). Within GC B cell populations, the LZ GC B cells possessed significantly more Cbl and Cbl-b protein but not mRNA compared to the DZ B cells (**Figures 1C, 1D, S1C** and **S1D**). These results indicate that Cbl proteins are post-transcriptionally and dynamically modulated during the GC reaction.

Ablation of Cbl proteins in GC B cells impairs antibody affinity maturation

We then generated *Cbl*$^{fl/fl}$ *Cbl-b*$^{-/-}$ *IgCγ-cre* transgenic (tg) mice in which the *IgCγ-cre* allele drove Cre recombinase expression in GC B cells so that only GC B cells (perhaps some activated B cells) carried the Cbl and Cbl-b double null (termed here as Cbl$^{-/-}$ Cbl-b$^{-/-}$) mutation, whereas other cells of the mice harbored the germline *cbl-b* mutation (Casola et al., 2006; Chiang et al., 2000; Naramura et al., 2002). Ablation of Cbl and Cbl-b proteins in GC B cells was confirmed by Western blot analysis and immunofluorescent staining (**Figures S2A** and **S2B**). Inspection of Cbl$^{-/-}$ Cbl-b$^{-/-}$ mice revealed normal development of B cells (**Figures S2C** and **S2D**). Compared to WT mice, the mutant mice produced similar levels of total anti-NP

(NP_{30}) antibodies of IgM and IgG1 isotypes initially, after immunization with (4-Hydroxy-3-Nitrophenyl)Acetyl-Keyhole Limpet Hemocyanin (NP-KLH); however, they displayed a significantly lower level of IgG1 at day 28 (**Figure 2A**). In addition to the antibody titer, $Cbl^{-/-}$ $Cbl\text{-}b^{-/-}$ mice exhibited impaired antibody affinity maturation, as the level of anti-NP_4 as well as the ratio of high affinity anti-NP (NP_4) vs total anti-NP (NP_{30}) IgG1 was severely impaired in the mutant mice compared to the WT controls (**Figures 2B** and **2C**). In addition, the mutant mice possessed slightly more IgM antibody-secreting cells (ASCs) against NP_{30} antigen. In contrast, they had markedly reduced numbers of total (anti-NP_{30}) as well as high affinity (anti-NP_4) IgG1 ASCs relative to their WT counterparts (**Figure 2D**). The discrepancy between the serum anti-NP_{30} antibody titers at day 14 (Figure 2A) and the numbers of anti-NP_{30} APCs at day 12 (Figure 2D) could be explained by that the formers reflect the accumulative antibodies produced by BM and peripheral ASCs, whereas the latters counted only the splenic ASCs present at the given date.

In T-cell dependent immune responses, ASCs or PCs are mostly derived from GC B cells. To examine whether the $Cbl^{-/-}$ $Cbl\text{-}b^{-/-}$ mutation affected the GC reaction, we analyzed the kinetics of GC B cell development during the course of immunization. At day 8 after immunization, WT and $Cbl^{-/-}$ $Cbl\text{-}b^{-/-}$ mice developed equal percentages of GC B cells; however, while WT mice exhibited a peak GC development at day 11 and declined GC B cell numbers thereafter, the mutant mice had a slow increase in GC B cells up to day 22 (**Figure 2E**). The altered kinetics of GC B cell development in the mutant mice could be partly attributed to a combinatory effect of expedited differentiation and reduced apoptosis, because $Cbl^{-/-}$ $Cbl\text{-}b^{-/-}$ GC B cells generated more plasma cells (see below) and expressed a lower number of active Caspase positive cells compared to the WT controls, respectively (**Figure 2F**). Cell cycle analysis revealed similar proportions of G1, S, and G2/M phase cells, indicating that the proliferation of GC B cells was not affected by the $Cbl^{-/-}$ $Cbl\text{-}b^{-/-}$ mutation (**Figure S3A**). In addition to the altered kinetics of GC B cell expansion, the mutant mice had a markedly lower number of GC B cells expressing a high affinity cell surface IgG1 BCR against NP antigen relative to the WT mice throughout the

course of immunization (**Figure 2G**). The influence on high affinity BCR-expressing GC B cells was not caused by IgCγ-Cre tg and appeared to be redundant between Cbl and Cbl-b, because IgCγ-Cre tg mice had normal numbers of total and high affinity GC B cells, and ablation of Cbl or Cbl-b alone exhibited only a relatively mild effect on the numbers of high affinity NP-binding GC B cells compared to the $Cbl^{-/-}$ $Cbl\text{-}b^{-/-}$ mutants (**Figure S3B and S3C**). Together, our results indicate that Cbl proteins control antibody affinity maturation and to less extent the total antibody production. In addition, the data also suggest that this regulation occurs at the stage of GC B cells.

Cbl proteins regulate GC selection for high affinity BCR-expressing B cells

Deficiency in generating high affinity antibody producing cells could be a result of impaired SHM or lack of selection for high affinity B cells in the GC. To distinguish these two possibilities, we first analyzed SHM in IgH genes in GC B cells. We isolated $Ig\lambda1^{+}$ GC B cells from NP-KLH immunized mice by FACS sorting at day 14 postimmunization and examined SHM in Ig V_H186.2 by DNA sequencing according to the previous publication (Dominguez-Sola et al., 2012) (**Figure S4A**). We found that while all (20/20) V_H186.2 genes isolated from WT GC B cells carried at least one mutation (range: 1-15 mutations), about ~85% (17/20) of V_H186.2 genes from $Cbl^{-/-}$ $Cbl\text{-}b^{-/-}$ GC B cells were mutated (range: 1-9 mutations) (**Figure 3A** and **3B**). In addition, V_H186.2 genes from WT GC B cells carried five replacement mutations/clone and 65% (13/20) of V_H186.2 genes harbored a tryptophan to leucine mutation at position 33 (W33L) (**Figure 3C**), a mutation known to encode a high affinity BCR to NP when paired with a Igλ1 light chain. In contrast, V_H186.2 genes from $Cbl^{-/-}$ $Cbl\text{-}b^{-/-}$ B cells possessed merely two replacement mutations per clone on average and only 15% (3/20) of clones carried a W33L mutation. Analysis of the replacement vs silent mutations (R/S ratio) in V_H186.2 genes revealed that while the V_H genes from WT GC B cells had undergone strong selection (R/S = 5), those from $Cbl^{-/-}$ $Cbl\text{-}b^{-/-}$ B cells exhibited an R/S ratio equivalent to that expected for the random mutation (R/S = 2) (**Figure 3D**). The frequencies of the silent

mutations in V_H186.2 genes were comparable between WT and Cbl$^{-/-}$ Cbl-b$^{-/-}$ B cells (**Figure 3B**), indicating that the SHM *per se* is not affected by the Cbl$^{-/-}$ Cbl-b$^{-/-}$ mutation. To ascertain that the above phenomenon in V_H186.2 genes indeed reflected that in NP-specific BCRs, we also compared SHM in V_H186.2 genes isolated from NP_{38}-binding GC B cells. Consistent with that observed in Ig$\lambda 1^+$ GC B cells, the number of V_H186.2 genes carrying a W33L mutation was also significantly reduced in the mutant NP-specific GC B cells compared to WT controls (**Figure S4B** and **S4C**).

To directly examine whether Cbls regulated cellular selection of high affinity BCR-expressing cells inside GCs, we compared the kinetics of high affinity NP (NIP_5) and total NP (NP_{38})-binding GC B cell development at different time points upon NP-KLH immunization (**Figure 3E**). At day 8 after immunization, WT mice had approximately 20% of NIP_5-binding and 31% NP_{38}-binding GC B cells, indicating that approximately 65% of total NP-specific GC B cells express a high affinity BCR as defined by NIP_5-binding capability. By day 14, the ratio of NIP_5 vs NP_{38}-binding GC B cells increased to more than 90%, indicating that the high affinity NP specific B cell population is selectively expanded within total NP specific GC B cells. In contrast to WT mice, Cbl$^{-/-}$ Cbl-b$^{-/-}$ mice possessed relatively lower numbers of NIP_5 and NP_{38}-binding GC B cells at day 8 (average 5% and 9%, respectively), equivalent to approximately 61% of NIP_5-binding cells among total NP_{38}-binding cells. However, by day 14 this ratio only increased slightly to less than 70%, indicating that the selection for NIP_5-binding cells is severely impaired in the mutant mice.

Taken together, the above data demonstrate that Cbls are required for the selection of high affinity BCR expressing B cells during GC reaction. However, they appear to be dispensable for the regulation of SHM in GC B cells.

The Cbl$^{-/-}$ Cbl-b$^{-/-}$ mutation expedites GC B cell differentiation to PCs

During affinity maturation, GC B cells undergo multiple cycles of proliferation and SHM in the DZ and selection and differentiation to PCs and memory B cells in the LZ (Meyer-Hermann et al., 2012; Victora et al., 2010). Disruption of these cycles may impair affinity-driven selection of GC B cells (Allen et al., 2007; Mesin et al., 2016). To understand the mechanisms by which Cbl proteins regulate GC affinity selection, we examined whether the $Cbl^{-/-}$ $Cbl\text{-}b^{-/-}$ mutation affected the development of DZ and LZ GC B cells or the differentiation dynamics of GC B cells to PCs. The DZ and LZ architecture and B cell populations in the immunized $Cbl^{-/-}$ $Cbl\text{-}b^{-/-}$ mice appeared to be normal (**Figure S5A** and **S5B**). However, $B220^{+}$ $GL7^{hi}$ Fas^{hi} GC B cells in $Cbl^{-/-}$ $Cbl\text{-}b^{-/-}$ mice possessed significantly more plasma cell precursor-like cells that downregulated Bcl6 and slightly upregulated CD138 (**Figure S5C**), suggesting that the $Cbl^{-/-}$ $Cbl\text{-}b^{-/-}$ mutation expedites GC B cells to PC differentiation.

To examine whether the $Cbl^{-/-}$ $Cbl\text{-}b^{-/-}$ mutation affected GC B cell differentiation, we performed BrdU labeling experiment to determine whether GC B cell development into PCs was increased in the mutant mice. At day 12 after immunization, in both WT and $Cbl^{-/-}$ $Cbl\text{-}b^{-/-}$ mice approximately 90% of GC B cells incorporated BrdU after twenty-four hours of BrdU labeling (**Figure S6A**), consistent with previous findings that GC B cells are vigorously proliferating. In contrast, the mutant mice generated 50% more $BrdU^{+}$ PCs as compared to WT mice (17% vs 11%) during the same period, which was equivalent to the genesis of 6,000 PCs/hour/spleen in $Cbl^{-/-}$ $Cbl\text{-}b^{-/-}$ mice compared to 4,000/hour/spleen in WT controls (**Figures 4A** and **4B**). These $BrdU^{+}$ PCs were mostly newly generated from NP-KLH activated B cells, rather than derived from spontaneous immune responses or existing PC and plasma blast proliferation, because twenty-four hours BrdU labeling of un-immunized WT and $Cbl^{-/-}$ $Cbl\text{-}b^{-/-}$ mice produced only 1-2% of $BrdU^{+}$ PCs (**Figure S6B**). Given that the mutant mice had less GC B cells than WT controls at day 12 after immunization (**Figure 2E**), increased PC genesis in $Cbl^{-/-}$ $Cbl\text{-}b^{-/-}$ mice is consistent with the idea that Cbl proteins are responsible for retaining GC B cells in the DZ-LZ cycle and preventing them from differentiation into PCs.

To directly assess the effect of Cbls on the fate choice of B cells in developing GCs in the context of affinity selection, we examined the development of high affinity NP-specific GC B cells and PCs upon inducible ablation of Cbls. We transferred B cells from ER-Cre tg (Control) or $Cbl^{fl/fl}$ Cbl-$b^{-/-}$ ER-Cre tg (termed $Cbl^{-/-}$ Cbl-$b^{-/-ERCre}$) mice into μMT recipient mice and immunized the chimeric mice with NP-KLH so that the donor B cells could enter and initiate GC reaction. We then deleted Cbls by tamoxifen at day 7 after immunization, at which stage about 60% of NP specific B cells already acquired a high affinity BCR (**Figure 3E**), and analyzed NIP_5-binding GC B cells and PCs at day 12 by flow cytometry. Mice ablated Cbls showed a marked reduction in the number of NIP_5-binding GC B cells; however, the total number of GC B cells was only moderately reduced compared to that in controls (**Figure 4C**). Consistently, Cbl ablation led to significant increases in the numbers of total and NIP_5-binding PCs relative to mice without Cbl deletion (**Figure S6C** and **S6D**). Given that high affinity PCs are mostly generated through GC reaction, concomitant reduction in NIP_5-binding GC B cells and increase in NIP_5-binding PCs supports the idea that loss of Cbls facilitates the high affinity GC B cells to choose the PC fate and differentiate into PCs.

Differentiation of GC B cells to PCs is influenced by CD40 and the BCR (Krautler et al., 2017). To determine whether Cbl control the PC differentiation program via differentiation to PCs *in vitro*. Stimulation of $Cbl^{-/-}$ Cbl-$b^{-/-}$ naïve B cells from $Cbl^{fl/fl}$ Cbl-$b^{-/-}$ Mb1-Cre tg mice with either membrane-bound CD40L expressed on 40LB feeder cells or soluble anti-CD40 generated significantly more $B220^{-}CD138^{+}$ and $B220^{+}$ $CD138^{+}$ cells (**Figures 4D** and **S6E**). These cells appeared to be PCs or plasma blast-like cells because they expressed intracellular Ig, upregulated Irf4, and downregulated Bcl6 (**Figure S6F**). Similarly, culture of freshly isolated $Cbl^{-/-}$ Cbl-$b^{-/-}$ GC B cells on CD40LB feeders also generated more $B220^{+}CD138^{+}$ plasma blast-like cells relative to WT controls (**Figure 4E**). In contrast, anti-IgM stimulation alone produced comparable numbers of $B220^{+}CD138^{+}$ cells from the mutant and WT B cells, suggesting that BCR signaling induced PCs is not enhanced by the $Cbl^{-/-}$ Cbl-$b^{-/-}$

mutation (**Figure S6E**). Neither CD40 nor BCR-induced proliferation of B cells was affected by the Cbl$^{-/-}$ Cbl-b$^{-/-}$ mutation (**Figure S6G**). Together, these data indicate that ablation of Cbl proteins does not affect CD40 or BCR induced GC B cell proliferation but rather expedites CD40-induced B cell differentiation into PCs.

The frequency of B cell differentiation into PCs increases with each cell division cycle (Hasbold et al., 2004). To study the influence of the Cbl$^{-/-}$ Cbl-b$^{-/-}$ mutation on PC differentiation in each cell division, we labeled naïve WT and Cbl$^{-/-}$ Cbl-b$^{-/-}$ B cells with CellTrace, stimulated them with 40LB feeder cells, and then examined PC differentiation in different divisions of proliferating B cells by monitoring both the Irf4 and CD138 expression. Consistent with the above finding, ablation of Cbls did not affect the rate of B cell division; however, the mutant B cells generated 50% more Irf4^{hi} cells than WT controls in the third and fourth cell division (**Figure 4F**). A similar increase in CD138^{+} cells was also found in the Cbl$^{-/-}$ Cbl-b$^{-/-}$ compared to the WT B cell culture (**Figure S6H**). These findings together indicate that, while still maintaining vigorous cell division, loss of Cbls induces more B cells to exit B cell fate and turn on the PC differentiation program in each cell division.

The Cbl$^{-/-}$ Cbl-b$^{-/-}$ mutation enhances the expression of Irf4 protein but not mRNA in GC B cells

The identities of GC B cells and PCs are respectively controlled by Bcl6 and Blimp1. Irf-4 provides another layer of regulation by repressing *Bcl6* and promoting *Blimp1* gene transcription (Basso and Dalla-Favera, 2015). To elucidate how the Cbl$^{-/-}$ Cbl-b$^{-/-}$ mutation affected the GC B cell differentiation program, we compared the gene expression profiles of GC B cell and PC identity genes in WT and Cbl$^{-/-}$ Cbl-b$^{-/-}$ GC B cells at day 12 after immunization. RNA-seq analysis revealed that the expression of ~900 genes was decreased and ~50 genes increased for at least two-fold in Cbl$^{-/-}$ Cbl-b$^{-/-}$ GC B cells as compared to WT controls (**Figure S7A**); however, this analysis revealed a slightly lower expression of several known GC B cell or PC identity genes such as *Bcl6*, *Bach2, Irf4,* and *Aicda* (**Figure S7B**). qPCR analysis confirmed that while the expression of *Bcl6*, *Bach2*, and *Aicda* was slightly reduced, the expression

of PC identity gene *Irf4* was not increased in the mutants compared to WT GC B cells (**Figure 5A**). Despite this observation, the mutant GC B cells elevated the expression of multiple genes related to RNA processing and protein translation and secretion involved in PC function (**Figures 5B and S7A**), suggesting that some mutant B cells already initiate the PC differentiation program.

To determine whether the $Cbl^{-/-}$ $Cbl\text{-}b^{-/-}$ mutation influenced the PC development program at the protein level, we examined CD40 and BCR signaling, as well as the levels of Bcl6 and Irf4 proteins in GC B cells. We found that activation of CD40 or BCR signaling pathways, including canonical NF-κB, AKT, S6K, and ERK, was not altered by the $Cbl^{-/-}$ $Cbl\text{-}b^{-/-}$ mutation (**Figures ES1A-C**). In contrast, the expression of Irf4 protein was markedly increased in freshly isolated mutant GC B cells compared to the controls (**Figure 5C**). To gain insight into the expression of Irf4 and Bcl6 during GC B cell differentiation at the single cell level, we examined intracellular Bcl6 and Irf4 in developing GC B cells by flow cytometry. In WT mice, a majority of GC ($B220^{+}$ Fas^{hi} $GL7^{hi}$) B cells expressed a high level of Bcl6 ($Bcl6^{hi}$), whereas only approximately 10% of GC B cells exhibited reduced level of Bcl6 ($Bcl6^{lo}$) and about half of them simultaneously had more Irf4 protein ($Bcl6^{lo}$ $Irf4^{hi}$), a population that might represent PC precursors (**Figure 5D**). Stimulation of CD40 and BCR for 3 hours significantly increased the $Bcl6^{lo}$ $Irf4^{hi}$ subset to ~40% of the total GC B population (**Figure 5E**). In contrast to WT mice, $Cbl^{-/-}$ $Cbl\text{-}b^{-/-}$ mice already possessed significantly more (15%) $Bcl6^{lo}$ $Irf4^{hi}$ GC B cells in the absence of any stimulation, and CD40 and BCR stimulation boosted the $Bcl6^{lo}Irf4^{hi}$ population to more than ~50% of total GC B cells (**Figures 5D and 5E**). Western blot analysis confirmed that Irf4 protein was indeed elevated in $Cbl^{-/-}$ $Cbl\text{-}b^{-/-}$ GC B cells compared to WT cells with or without CD40 and BCR stimulation **(Figure 5F**). This result, along with the mRNA expression data, indicates that Cbl proteins do not affect the major signaling pathways downstream of CD40 or the BCR. Instead, they may retain GC B cells fate by suppressing the expression of Irf4 protein rather than *Irf4* transcription.

Cbls promote nuclear Irf4 ubiquitination and degradation

Cbl proteins are known cytosolic E3 ubiquitin ligases, whereas Irf4 is a transcription factor that functions mainly in the nucleus. We therefore examined at which subcellular location Cbl proteins exert their regulatory function on Irf4. Confocal microscopy analysis showed that Irf4 was barely detectable in freshly isolated WT GC B ($B220^{+}$ $GL7^{hi}$ Fas^{hi}) cells and significantly accumulated in the nucleus after CD40 and BCR stimulation. In contrast, a significant proportion of $Cbl^{-/-}$ $Cbl\text{-}b^{-/-}$ GC B cells already possessed a high level of nuclear Irf4 in the absence of any stimulation (**Figures 6A and 6B**). In agreement with this observation, Western blot analysis confirmed that Irf4 was expressed in both cytosol and nucleus, with the mutant GC B cells expressing several folds more Irf4 than WT cells in the nucleus even in the absence of any stimulation (**Figure 6C**). As for Cbls, in freshly isolated WT GC B cells both Cbl and Cbl-b were expressed in the cytosol and nucleus in the absence of CD40 stimulation, with Cbl more strongly in cytosol and Cbl-b in the nucleus (**Figure 6D**). CD40 and BCR stimulation for one hour significantly diminished Cbl-b and for three hours reduced both Cbl-b and Cbl in the nucleus. The stimulation concomitantly increased the level of nuclear Irf4 (**Figure 6D**), suggesting that nuclear Cbl proteins eradicate Irf4 in GC B cells.

To determine whether Cbl proteins regulated Irf4 expression by promoting Irf4 ubiquitination, we co-expressed Irf4 with either Cbl or Cbl-b in 293T cells and examined Irf4 association with, and ubiquitination by, Cbl or Cbl-b by immunoprecipitation and Western blot analysis. Irf4 associated with, and became ubiquitinated by, either Cbl or Cbl-b in 293T cells (**Figures 6E and 6F**). The association of Irf4 with Cbl and Cbl-b in freshly isolated WT GC B cells, as well as its ubiquitination in WT but not in $Cbl^{-/-}$ $Cbl\text{-}b^{-/-}$ iGC B cells, was confirmed by co-immunoprecipitation and Western blot hybridization (**Figure 6G and 6H**). Thus, the observed dynamic change of Irf4 expression in GC LZ B cells is at least partly regulated by Cbl-dependent Irf4 ubiquitination and degradation.

Lack of Cbl ubiquitin ligase activity or increase in Irf4 expression is sufficient to impair GC affinity selection

The above results suggest a hypothesis that the elevated level of Cbls in GC B cells removes Irf4 by promoting Irf4 ubiquitination, consequently allowing continuation of GC cycle until high affinity BCRs are acquired. If this is the case, we expected that inactivation of Cbl ubiquitin ligase activity or increased Irf4 expression in GC B cells impairs antibody affinity maturation. To examine whether Cbl ubiquitin ligase activity was required for antibody affinity maturation, we bred $Cbl^{fl/fl}$ mice to IgCγ-Cre tg and Cbl-$b^{C373A/C373A}$ mice, the latter expressed a mutant Cbl-b whose ubiquitin ligase activity was inactivated by a cysteine to alanine mutation at position 373 of the Cbl-b (Oksvold et al., 2008). The resulting $Cbl^{fl/fl}$ Cbl-$b^{-/C373A}$ IgCγ-Cre tg (termed $Cbl^{-/-}$ Cbl-$b^{-/C373A}$) mice were immunized with NP-KLH. The development of high affinity GC B cells and PCs were examined by flow cytometry and ELISPOT, respectively. $Cbl^{-/-}$ Cbl-$b^{-/C373A}$ mice recapitulated GC B cell phenotypes found in $Cbl^{-/-}$ Cbl-$b^{-/-}$ mice, as they produced a slightly lower number of GC B cells compared to $Cbl^{fl/fl}$ Cbl-$b^{-/+}$ IgCγ-Cre tg and WT controls at day 12 after immunization (**Figure 7A** and **S9A**). In addition, the numbers of high affinity anti-NP (NP_8) GC B cells as well as anti-NP_8 IgG1 secreting PCs were all reduced in the mutant mice relative to the controls (**Figures 7B**, **7C** and E**S2A**).

To determine whether increased Irf4 protein was sufficient to abolish antibody affinity maturation, we ectopically expressed Irf4 in WT hematopoietic stem cells by a retroviral vector and generated BM chimeras (termed Irf4-MSCV BM mice). Expression of the transgenic Irf4 was confirmed by Western blot analysis (**Figure ES2B**). These mice were then immunized with NP-KLH, and selection of high affinity NP-binding GC B cells and PCs was analyzed by flow cytometry. Similar to that found in $Cbl^{-/-}$ Cbl-$b^{-/-}$ and $Cbl^{-/-}$ Cbl-$b^{-/C373A}$ mice, in IRrf-MSCV BM chimeras the transgene Irf4 expressing (Irf4-MSCV) B cells generated a slightly lower number of GC B cells at day 12 compared to empty retrovirus (MIGR-MSCV) infected B cells (**Figure 7D**), indicating that Irf4-overexpressing B cells can enter GC reaction. However, the

production of high affinity anti-NP_8 IgG1 expressing GC B cells was impaired in the mutant (Irf4-MSCV, GFP^+) but not in WT controls (MIGR-MSCV, GFP^+) (**Figure 7E**). The numbers of PCs generated from Irf4-MSCV infected B cells were consistently increased as compared to empty vector infected cells (**Figure 7F**).

Together, these results indicate that lack of ubiquitin ligase activity of Cbls or excessive Irf4 expression is sufficient to abolish the development of high affinity GC B cells.

DISCUSSION

Selective expansion of high affinity BCR-expressing B cells in GCs is a critical step in antibody affinity maturation. We found that Cbls play an indispensable role in this regulation, as ablation of Cbls in GC B cells selectively impaired the development of GC B cells expressing high but not low affinity BCRs. Loss of Cbls in GC B cells did not significantly alter the efficiency of SHM *per se*, but rather impeded the clonal expansion of high affinity B cells in GCs. Since inactivation of Cbl ubiquitin ligase activity was sufficient to recapitulate this GC phenotype, our studies support the notion that Cbls define an ubiquitination-dependent regulatory pathway that enforces affinity-driven clonal selection of high affinity GC B cells.

It is generally envisioned that high affinity BCRs facilitate clonal expansion and selection of GC B cells via two modes of regulation. First, high affinity BCRs may drive more vigorous cell proliferation, because they elicit stronger BCR signaling than low affinity BCRs. However, this proposition has received conflicting evidence, as attenuated rather than enhanced BCR signaling is favorable for GC B cell expansion and high affinity BCRs tend to cease GC B cell fate and initiates PC differentiation (Khalil et al., 2012; Krautler et al., 2017). As an alternative to the signaling role of the BCR in GC affinity selection, high affinity BCRs are thought to capture more antigen than BCRs with inferior affinity, thus giving high affinity B cells the advantage of competing for the help of Tfh cells, mainly via the increased expression of CD40L (Gitlin et al., 2014; Liu et al., 2015). How B cells interpret BCR

affinity cues differently since the same signals control both the mitotic and differentiation pathways of GC B cells is unclear. In our studies, we found that ablation of Cbls expedited GC B cell differentiation, but not proliferation upon CD40 and/or BCR stimulation. This finding thus puts Cbls at the branch of signaling pathway to prevent the B cell differentiation rather than proliferation. In line with this view, we observed that the $Cbl^{-/-}$ $Cbl\text{-}b^{-/-}$ mutation did not affect CD40 and BCR induced mitotic signaling such as AKT, S6K, ERKs, and canonical NF-κB. Instead, it resulted in the accumulation of Irf4 protein in GC B cells. We also found that in B cells Cbls promote Irf4 ubiquitination. CD40 and BCR stimulation decreased the expression of Cbls and conversely increased the expression of Irf4 in GC B cells. Finally, ablation of Cbls in GC B cells using ER-Cre inducible system preferentially facilitated high affinity B cells to terminate the GC fate and differentiate into PCs. Taken together, theses findings lead to a model wherein by clearing Irf4 protein rather than regulating the mitotic signaling pathways, Cbls enable CD40 and BCR signals to promote GC B cell proliferate without activating the PC differentiation program. This regulation can be reversed in high affinity GC B cells in which strong CD40 and BCR signaling generated by the high affinity BCRs cue decreases the expression of Cbls, leading to increased amount of Irf4 and differentiation of these cells into PCs.

The fates of GC B cells and PCs are determined by transcription factors Bcl6, Irf4, and BLIMP (Basso and Dalla-Favera, 2015; Shapiro-Shelef and Calame, 2005). However, a recent transcriptome study revealed that transcription of *Bcl6* is abruptly decreased whereas that of *Irf4* and *pmdr1* is abruptly increased in plasmablasts, hence raising a question as to what is the initial "push" that drives the transition of this transcriptional network from the equilibrium state of GC B cells to that of PCs (Shi et al., 2015). Our data reveal that in WT mice a small population of GC B cells downregulated Bcl6 and upregulated Irf4 ($Bcl6^{lo}Irf4^{hi}$). Triggering of CD40 and BCR for a short period increased this cell subset, suggesting that these cells represent emerging plasmablasts or plasma cell precursors. Development of

this subset appeared to be controlled by Cbls, because they were significantly increased in the GCs of Cbl$^{-/-}$ Cbl-b$^{-/-}$ mice. In GC B cells, we showed that Cbls ubiquitinated Irf4. Strong CD40 and BCR stimulation decreased the expression of Cbl proteins and concomitantly increased the expression of Irf4. We therefore propose that relief of Irf4 from Cbl-mediated ubiquitination upon strong CD40 and/or BCR triggering is the earliest PC fate commitment event occurring in the LZ GC B cells, preceding the conversion of transcriptomes from the state of GC B cells to that of PCs. This of course will not refute the role of CD40 in promoting *Irf4* gene transcription, which may be compromised in LZ B cells at the Irf4 protein level until Cbls are degraded.

Previous studies have shown that selection of high affinity GC B cells depends on the transcription factors NFκB, Myc, and Foxo1, in a B cell-intrinsic fashion. Both Myc and canonic NFκB are expressed or activated in a small subset of LZ GC B cells (Calado et al., 2012; De Silva and Klein, 2015; Dominguez-Sola et al., 2015; Heise et al., 2014). Ablation of *Myc*, *rel* or *relb* genes, respectively, in GC B cells results in the collapse of the GC reaction, because these factors are required for the maintenance of the GC reaction by facilitating LZ to DZ circulation. Foxo1 is required for sustaining the DZ program, as inactivation of *Foxo1* gene disrupts the expansion of DZ B cells possibly by dysregulating the function of the transcription factor Batf (Inoue et al., 2017). In contrast to the above regulations, Cbls control GC affinity maturation by determining the time when a GC B cell is allowed to enter the PC pool. In this regard, Cbls seem to represent a new regulation that controls the exit checkpoint of the DZ-LZ cycle, consequently contributing to BCR affinity selection. It will be interesting to determine whether this mechanism also contributes to the recently described temporal switch in the differential output of memory B cells and PCs during the GC reaction (Weisel et al., 2016).

Selection of high affinity B cells occurs in the GC LZ where BCR affinity cues can be assessed via interaction with antigen presented on follicular dendritic cells

(Heesters et al., 2014). Our findings that the expression of Cbls is markedly increased in GC LZ compared to DZ B cells at the protein but not at the mRNA level, and that CD40 and BCR signals reduce the expression of Cbl proteins, raise an interesting question as to how the expression of Cbls is spatially and temporally controlled during the GC DZ-LZ cycle. CD40 is known to activate RING-domain containing Trafs or cIAPs, both of which regulate their respective downstream signaling molecules by ubiquitination (Elgueta et al., 2009). Along this line, at least Traf 6 and Traf 2 have been shown to associate with Cbl-b (Elgueta et al., 2009). Alternatively, CD40 signal could modulate the translation of Cbl proteins through a microRNA dependent mechanism. Consistent with this speculation, it has been found that CD40 stimulation enhances the expression of multiple microRNAs among which miR155 may influence Cbl-b expression in B cells (Loeb et al., 2012; Vigorito et al., 2007). Nevertheless, it will be interesting to investigate whether modulation of the Cbl pathway can be used as a strategy to improve the clinical benefit such as the efficiency of vaccination in future.

STAR★METHODS

Detailed methods are provided in the online version of this paper and include the following:

- KEY RESOURCES TABLES
- CONTACT FOR REAGENTS AND RESOURCE SHARING
- EXPERIMENTAL MODLE AND SUBJECT DETAILS
    - Mice
- METHOD DETAILS
    - Plasmid, cell line and culture
    - Immunization and GC B cell purification
    - Flow cytometric analysis and cell sorting
    - qPCR and RNA-seq analysis

- Immunofluorescence
- $IgV_H186.2$ gene isolation and DNA sequencing
- ELISPOT and ELISA
- Immunoprecipitation and Immunoblot analysis
- Bone marrow and spleen B cell chimeric mice
- Cell division and differentiation assay

- STATISTICAL ANALYSIS

SUPPLEEMENTAL INFORMATION

Supplemental information includes ten figures.

ACKNOWLEDGEMENTS

We thank F. Huang (Fudan University Medical College, Shanghai, China) for MSCV-IκB-GFP reporter, R. Chen (IRCM, Montreal, Canada) for HA-Ubiqutin vector, and J. Di Noia, T. Möröy, W.-K. Suh, and A. Veillette for comments. Supported by The Canadian Institute of Health Research (CIHR) Operating Grant (MOP142279) and A. Aisenstadt Chair Fund to H. G.; Chinese Scholarship Council Ph.D. training grants to X. L. and H. J. T.; NCI-NIH R21 CA175461 to U. K.; National Health and Medical Research Grant (1101318) to W. Y. L.; The CAS/SAFEA for International Partnership Program for Creative Research Teams to F. J. H. and H. G; and a NSHLIJ Institutional Fund to Y. R. Z.

AUTHOR CONTRIBUTIONS

X. L. did mouse, biochemical, and flow cytometric analyses; A. G, H. J. T., L. Y. G., and Y. L. contributed to the design and method refinement of biochemistry and flow cytometric analyses and daily discussion; D. K. generated 40LB feeder cells; V. C., contributed to bioinformatics analysis; U. K. contributed to Irf4 analysis and manuscript writing; W. Y. L. generated Cbl-b^{C373A} mice; F. J. H. contributed to discussion; and Y. R. Z. contributed to fluorescent imaging analysis, experiment design, and manuscript writing; All authors had editorial input.

REFERENCES

Allen, C.D., Okada, T., and Cyster, J.G. (2007). Germinal-center organization and cellular dynamics. Immunity *27*, 190-202.

Bannard, O., and Cyster, J.G. (2017). Germinal centers: programmed for affinity maturation and antibody diversification. Curr Opin Immunol *45*, 21-30.

Basso, K., and Dalla-Favera, R. (2012). Roles of BCL6 in normal and transformed germinal center B cells. Immunol Rev *247*, 172-183.

Basso, K., and Dalla-Favera, R. (2015). Germinal centres and B cell lymphomagenesis. Nat Rev Immunol *15*, 172-184.

Berek, C., Berger, A., and Apel, M. (1991). Maturation of the immune response in germinal centers. Cell *67*, 1121-1129.

Calado, D.P., Sasaki, Y., Godinho, S.A., Pellerin, A., Kochert, K., Sleckman, B.P., de Alboran, I.M., Janz, M., Rodig, S., and Rajewsky, K. (2012). The cell-cycle regulator c-Myc is essential for the formation and maintenance of germinal centers. Nat Immunol *13*, 1092-1100.

Casola, S., Cattoretti, G., Uyttersprot, N., Koralov, S.B., Seagal, J., Hao, Z., Waisman, A., Egert, A., Ghitza, D., and Rajewsky, K. (2006). Tracking germinal center B cells expressing germ-line immunoglobulin gamma1 transcripts by conditional gene targeting. Proc Natl Acad Sci U S A *103*, 7396-7401.

Chiang, Y.J., Kole, H.K., Brown, K., Naramura, M., Fukuhara, S., Hu, R.J., Jang, I.K., Gutkind, J.S., Shevach, E., and Gu, H. (2000). Cbl-b regulates the CD28 dependence of T-cell activation. Nature *403*, 216-220.

Crotty, S. (2011). Follicular helper CD4 T cells (Tfh). Annu Rev Immunol *29*, 621-663.

De Silva, N.S., and Klein, U. (2015). Dynamics of B cells in germinal centres. Nat Rev Immunol *15*, 137-148.

Dominguez-Sola, D., Kung, J., Holmes, A.B., Wells, V.A., Mo, T., Basso, K., and Dalla-Favera, R. (2015). The FOXO1 Transcription Factor Instructs the Germinal Center Dark Zone Program. Immunity *43*, 1064-1074.

Dominguez-Sola, D., Victora, G.D., Ying, C.Y., Phan, R.T., Saito, M., Nussenzweig, M.C., and Dalla-Favera, R. (2012). The proto-oncogene MYC is required for selection in the germinal center and cyclic reentry. Nat Immunol *13*, 1083-1091.

Dufaud, C.R., McHeyzer-Williams, L.J., and McHeyzer-Williams, M.G. (2017). Deconstructing the germinal center, one cell at a time. Curr Opin Immunol *45*, 112-118.

Elgueta, R., Benson, M.J., de Vries, V.C., Wasiuk, A., Guo, Y., and Noelle, R.J. (2009). Molecular mechanism and function of CD40/CD40L engagement in the immune system. Immunol Rev *229*, 152-172.

Gitlin, A.D., Shulman, Z., and Nussenzweig, M.C. (2014). Clonal selection in the germinal centre by regulated proliferation and hypermutation. Nature *509*, 637-640.

Han, Y.C., Park, C.Y., Bhagat, G., Zhang, J., Wang, Y., Fan, J.B., Liu, M., Zou, Y., Weissman, I.L., and Gu, H. (2010). microRNA-29a induces aberrant self-renewal capacity in hematopoietic progenitors, biased myeloid development, and acute myeloid leukemia. J Exp Med *207*, 475-489.

Hasbold, J., Corcoran, L.M., Tarlinton, D.M., Tangye, S.G., and Hodgkin, P.D. (2004). Evidence from the generation of immunoglobulin G-secreting cells that stochastic mechanisms regulate lymphocyte differentiation. Nat Immunol *5*, 55-63.

Heesters, B.A., Myers, R.C., and Carroll, M.C. (2014). Follicular dendritic cells: dynamic antigen libraries. Nat Rev Immunol *14*, 495-504.

Heise, N., De Silva, N.S., Silva, K., Carette, A., Simonetti, G., Pasparakis, M., and Klein, U. (2014). Germinal center B cell maintenance and differentiation are controlled by distinct NF-kappaB transcription factor subunits. J Exp Med *211*, 2103-2118.

Huang, F., and Gu, H. (2008). Negative regulation of lymphocyte development and function by the Cbl family of proteins. Immunol Rev *224*, 229-238.

Inoue, T., Shinnakasu, R., Ise, W., Kawai, C., Egawa, T., and Kurosaki, T. (2017). The transcription factor Foxo1 controls germinal center B cell proliferation in response to T cell help. J Exp Med *214*, 1181-1198.

Jacob, J., Kelsoe, G., Rajewsky, K., and Weiss, U. (1991). Intraclonal generation of antibody mutants in germinal centres. Nature *354*, 389-392.

Jang, I.K., Cronshaw, D.G., Xie, L.K., Fang, G., Zhang, J., Oh, H., Fu, Y.X., Gu, H., and Zou, Y. (2011). Growth-factor receptor-bound protein-2 (Grb2) signaling in B cells controls lymphoid follicle organization and germinal center reaction. Proc Natl Acad Sci U S A *108*, 7926-7931.

Khalil, A.M., Cambier, J.C., and Shlomchik, M.J. (2012). B cell receptor signal transduction in the GC is short-circuited by high phosphatase activity. Science *336*, 1178-1181.

Kitaura, Y., Jang, I.K., Wang, Y., Han, Y.C., Inazu, T., Cadera, E.J., Schlissel, M., Hardy, R.R., and Gu, H. (2007). Control of the B cell-intrinsic tolerance programs by ubiquitin ligases Cbl and Cbl-b. Immunity *26*, 567-578.

Klein, U., Casola, S., Cattoretti, G., Shen, Q., Lia, M., Mo, T., Ludwig, T., Rajewsky, K., and Dalla-Favera, R. (2006). Transcription factor IRF4 controls plasma cell differentiation and class-switch recombination. Nat Immunol *7*, 773-782.

Krautler, N.J., Suan, D., Butt, D., Bourne, K., Hermes, J.R., Chan, T.D., Sundling, C., Kaplan, W., Schofield, P., Jackson, J.*, et al.* (2017). Differentiation of germinal center B cells into plasma cells is initiated by high-affinity antigen and completed by Tfh cells. J Exp Med *214*, 1259-1267.

Liu, D., Xu, H., Shih, C., Wan, Z., Ma, X., Ma, W., Luo, D., and Qi, H. (2015). T-B-cell entanglement and ICOSL-driven feed-forward regulation of germinal centre reaction. Nature *517*, 214-218.

Liu, Y.J., Joshua, D.E., Williams, G.T., Smith, C.A., Gordon, J., and MacLennan, I.C. (1989). Mechanism of antigen-driven selection in germinal centres. Nature *342*, 929-931.

Loeb, G.B., Khan, A.A., Canner, D., Hiatt, J.B., Shendure, J., Darnell, R.B., Leslie, C.S., and Rudensky, A.Y. (2012). Transcriptome-wide miR-155 binding map reveals widespread noncanonical microRNA targeting. Mol Cell *48*, 760-770.

Mesin, L., Ersching, J., and Victora, G.D. (2016). Germinal Center B Cell Dynamics. Immunity *45*, 471-482.

Meyer-Hermann, M., Mohr, E., Pelletier, N., Zhang, Y., Victora, G.D., and Toellner, K.M. (2012). A theory of germinal center B cell selection, division, and exit. Cell Rep *2*, 162-174.

Muramatsu, M., Kinoshita, K., Fagarasan, S., Yamada, S., Shinkai, Y., and Honjo, T. (2000). Class switch recombination and hypermutation require activation-induced cytidine deaminase (AID), a potential RNA editing enzyme. Cell *102*, 553-563.

Naramura, M., Jang, I.K., Kole, H., Huang, F., Haines, D., and Gu, H. (2002). c-Cbl and Cbl-b regulate T cell responsiveness by promoting ligand-induced TCR down-modulation. Nat Immunol *3*, 1192-1199.

Nojima, T., Haniuda, K., Moutai, T., Matsudaira, M., Mizokawa, S., Shiratori, I., Azuma, T., and Kitamura, D. (2011). In-vitro derived germinal centre B cells differentially generate memory B or plasma cells in vivo. Nat Commun *2*, 465.

Nutt, S.L., Hodgkin, P.D., Tarlinton, D.M., and Corcoran, L.M. (2015). The generation of antibody-secreting plasma cells. Nat Rev Immunol *15*, 160-171.

Oksvold, M.P., Dagger, S.A., Thien, C.B., and Langdon, W.Y. (2008). The Cbl-b RING finger domain has a limited role in regulating inflammatory cytokine production by IgE-activated mast cells. Mol Immunol *45*, 925-936.

Rajewsky, K. (1996). Clonal selection and learning in the antibody system. Nature *381*, 751-758.

Ramiscal, R.R., and Vinuesa, C.G. (2013). T-cell subsets in the germinal center. Immunol Rev *252*, 146-155.

Sander, S., Chu, V.T., Yasuda, T., Franklin, A., Graf, R., Calado, D.P., Li, S., Imami, K., Selbach, M., Di Virgilio, M.*, et al.* (2015). PI3 Kinase and FOXO1 Transcription Factor Activity Differentially Control B Cells in the Germinal Center Light and Dark Zones. Immunity *43*, 1075-1086.

Schwickert, T.A., Lindquist, R.L., Shakhar, G., Livshits, G., Skokos, D., Kosco-Vilbois, M.H., Dustin, M.L., and Nussenzweig, M.C. (2007). In vivo imaging of germinal centres reveals a dynamic open structure. Nature *446*, 83-87.

Sciammas, R., Shaffer, A.L., Schatz, J.H., Zhao, H., Staudt, L.M., and Singh, H. (2006). Graded expression of interferon regulatory factor-4 coordinates isotype switching with plasma cell differentiation. Immunity *25*, 225-236.

Shapiro-Shelef, M., and Calame, K. (2005). Regulation of plasma-cell development. Nat Rev Immunol *5*, 230-242.

Shapiro-Shelef, M., Lin, K.I., McHeyzer-Williams, L.J., Liao, J., McHeyzer-Williams, M.G., and Calame, K. (2003). Blimp-1 is required for the formation of immunoglobulin secreting plasma cells and pre-plasma memory B cells. Immunity *19*, 607-620.

Shi, W., Liao, Y., Willis, S.N., Taubenheim, N., Inouye, M., Tarlinton, D.M., Smyth, G.K., Hodgkin, P.D., Nutt, S.L., and Corcoran, L.M. (2015). Transcriptional profiling of mouse B cell terminal differentiation defines a signature for antibody-secreting plasma cells. Nat Immunol *16*, 663-673.

Shlomchik, M.J., and Weisel, F. (2012). Germinal center selection and the development of memory B and plasma cells. Immunol Rev *247*, 52-63.

Shulman, Z., Gitlin, A.D., Weinstein, J.S., Lainez, B., Esplugues, E., Flavell, R.A., Craft, J.E., and Nussenzweig, M.C. (2014). Dynamic signaling by T follicular helper cells during germinal center B cell selection. Science *345*, 1058-1062.

Victora, G.D., and Nussenzweig, M.C. (2012). Germinal centers. Annu Rev Immunol *30*, 429-457.

Victora, G.D., Schwickert, T.A., Fooksman, D.R., Kamphorst, A.O., Meyer-Hermann, M., Dustin, M.L., and Nussenzweig, M.C. (2010). Germinal center dynamics revealed by multiphoton microscopy with a photoactivatable fluorescent reporter. Cell *143*, 592-605.

Vigorito, E., Perks, K.L., Abreu-Goodger, C., Bunting, S., Xiang, Z., Kohlhaas, S., Das, P.P., Miska, E.A., Rodriguez, A., Bradley, A.*, et al.* (2007). microRNA-155 regulates the generation of immunoglobulin class-switched plasma cells. Immunity *27*, 847-859.

Weisel, F.J., Zuccarino-Catania, G.V., Chikina, M., and Shlomchik, M.J. (2016). A Temporal Switch in the Germinal Center Determines Differential Output of Memory B and Plasma Cells. Immunity *44*, 116-130.

STAR★METHODS

KEY RESOURCES TABLE

REAGENT or RESOURCE	SOURCE	IDENTIFIER

Antibodies		
anti-CD4 e450	Ebioscience/Thermo	Cat#48-0042-82
anti-CD8 e450	Ebioscience/Thermo	Cat#48-0032-82
anti-Gr1 e450	Ebioscience/Thermo	Cat#48-5931-82
anti-CD11c e450	Ebioscience/Thermo	Cat#48-0114-82
anti-CD11b e450	Ebioscience/Thermo	Cat#48-0112-82
anti-Ter119 e450	Ebioscience/Thermo	Cat#48-5921-82
anti-F4/80 e450	Ebioscience/Thermo	Cat#48-4801-82
anti-B220 e450	Ebioscience/Thermo	Cat#48-0452-82
anti-B220 PE-CY7	Ebioscience/Thermo	Cat#25-0452-82
anti-GL7 e450	Ebioscience/Thermo	Cat#48-5902-82
anti-GL7 FITC	Ebioscience/Thermo	Cat#53-5902-82
anti-IgM PE	Ebioscience/Thermo	Cat#12-5890-81
anti-CD23 PE-CY7	Ebioscience/Thermo	Cat#5-0232-81
anti-CD24 PE	Ebioscience/Thermo	Cat#12-0241-81
anti-CD93 APC	Ebioscience/Thermo	Cat#17-5892-82
anti-CXCR4 PE	Ebioscience/Thermo	Cat#12-9991-82
anti-Irf4 PE	Ebioscience/Thermo	Cat#12-9858-80
anti-B220 FITC	Ebioscience/Thermo	Cat#11-0452-82
Strepavidin PE-CY7	Ebioscience/Thermo	Cat#24-4317-82
anti-CD86	Ebioscience/Thermo	Cat#17-0862-81
anti-phospho-S6(S235/S236)	Ebioscience/Thermo	Cat#12-9007-42
anti-B220 APC	Biolegend	Cat#103212
anti-CD38 APC	Biolegend	Cat#102712
Alexa647 anti-BrdU	Biolegend	Cat#364108
anti-Ig□	Biolegend	Cat#407306
anti-Fas PE	BD	Cat#554258
anti-Fas PE-CY7	BD	Cat#557653
anti-IgG1 FITC	BD	Cat#553443
anti-IgD FITC	BD	Cat#553439
anti-CD21/CD35 FITC	BD	Cat#553818
Alexa647 anti-Bcl6	BD	Cat#561525
anti-CD138 PE	BD	Cat#553714
anti-CD35 Biotin	BD	Cat#553816
anti-CD138 e450	BD	Cat#562610
Alexa647 anti-AKT(p473)	BD	Cat#560343
Alexa647 anti-ERK1/2(pT202/pY204)	BD	Cat#612593
Purified anti-CD40	ENZO	Cat#ALX-805-046-C100
Purified anti-IgMF(ab)$_2$	Jasckson ImmunoResearch	Cat#115-006-020
anti-mouse Cbl	Santa Cruz	Cat#SC-170
anti-mouse Irf4	Santa Cruz	Cat#SC-6059
anti-LAMINB	Santa Cruz	Cat#SC-374015
anti-HA	Santa Cruz	Cat#SC-805
HRP conjugated anti-□-ACTIN	Abcam	Cat#AB49900
anti-Flag	Sigma	Cat#F1804-50UG
anti-Goat IgG HRP	Santa Cruz	Cat#SC-2020
anti-Rabbit IgG HRP	Cell Signaling	Cat#7074P2

anti-Mouse IgG HRP	Cell Signaling	Cat#7076P2
anti-Mouse Cbl-b	Cell Signaling	Cat#9498S
anti-Mouse IgG1 HRP	Thermo	Cat#A10551
anti-Mouse IgM HRP	Thermo	Cat#M31507
anti-□-Tubulin	Sigma	Cat#T4026-.2ML
PNA Biotin	Vector	Cat#B-1075
PNA FITC	Vector	Cat#FL-1071
Strepavidin Alexa488	Thermo	Cat#S-32354
Strepavidin Alexa568	Thermo	Cat#S-11226
Donkey anti-Goat Alexa594	Thermo	Cat#A-11058
Goat anti-Rabbit Alexa568	Thermo	Cat#A-11036
Bacterial and Virus Strains		
E.coli5□ competent cells	Thermo	Cat#18265017
Stbl2™ competent cells	Thermo	Cat#10268019
Stbl3™ competent cells	Thermo	Cat#C737303
Chemicals, Peptides, and Recombinant Proteins		
5-Fluorouracil	Sigma	Cat#F6627-5G
MG132	Sigma	Cat#C2211
NHS-Biotin	Thermo	Cat#21335
Recombinant mouse IL-4 protein	R&D	Cat#404-ML-050
Recombinant mouse SCF protein	R&D	Cat#455-MC-050
Recombinant mouse IL-6 protein	R&D	Cat#406-ML-025/CF
Recombinant mouse IL-3 protein	R&D	Cat#403-ML-050/CF
Celltrace Proliferation dye	Ebioscience/Thermo	Cat#C34557
SYBR Green qPCR Master Mix	Life Technology	Cat#4309155
NP_4-BSA	Bioresearch Technologies	Cat#N-5050L-10
NP_{30}-BSA	Bioresearch Technologies	Cat#N-5050L-10
rProtein G Agarose	Thermo	Cat#15920-010
Sheep Red Blood Cells	Innovative Research	Cat#IC100-0210
NP_{36}-KLH	Bioresearch Technologies	Cat#N-5060-25
1-Step™ Ultra TMB-ELISA Substrate Solution	Thermo	Cat#34029
Critical Commercial Assays		
FITC-BrdU kit	BD	Cat#559619
Nuclear Extract Kit	Active motif	Cat#40010
AEC Substrate Set	BD	Cat#551951
B cell negative selection kit	Stem cell	Cat#19854
CaspaseGlowTM FITC Active Caspase Staining Kit	Biodivision	Cat#A10551
Experimental Models: Cell Lines		
293T cell line	Laboratory of Gu	
Phoenix cell line	Laboratory of Gu	
40LB cell line	Laboratory of D. Kitamura	
Experimental Models: Organisms/Strains		
Cbl flox/flox conditional knockout mice	Laboratory of Gu	
Cbl-b germline knockout mice	Laboratory of Gu	

C□-cre mice	Laboratory of K. Rajewsky	
$Cblb^{C373A}$ mutation mice	Laboratory of W. Langdon	
C57BL/6 mice	The Jackson Laboratory	Stock#000664
B6.SJL mice	The Jackson Laboratory	Stock#002014
Rag1-/- mice	The Jackson Laboratory	Stock#002216
Oligonucleotides		
Cbl-b qPCR primer Forward: 5'-GGGGACGGCAATATCCTACAG-3' Reverse: 5'-TATAGCTCCGCCCATCAGGA-3'	IDT	N/A
Cbl qPCR primer Forward: 5'-CTCCTCCTTTGGCTGGTTGT-3' Reverse: 5'-TTCTCCGAGGGAATGGTTTGG-3'	IDT	N/A
Acida qPCR primer Forward: 5'-AAGGGACGGCATGAGACCTA-3' Reverse: 5'-AGCCAGACTTGTTGCGAAGG-3'	IDT	N/A
Irf4 qPCR primer Forward: 5'-AGGTCTGCTGAAGCCTTGGC-3' Reverse: 5'-CTTCAGGGCTCGTGGTC-3'	IDT	N/A
β-Actin qPCR primer Forward: 5'-CGATGCCCTGAGGCTCTT-3' Reverse: 5'-TGGATGCCACAGGATTCCA-3'	IDT	N/A
Gapdh qPCR primer Forward: 5'-TCGTCCCGTAGACAAAATGGT-3' Reverse: 5'-CGCCAAATACGGCCAAA-3'	IDT	N/A
Bcl6 qPCR primer Forward: 5'-TTTCTGGTTCACTGGCCTTGA-3' Reverse: 5'-CCTGCAGATGGAGCATGTTG-3'	IDT	N/A
Bach2 qPCR primer Forward: 5'-AGTAAGAACCGCATTGCAGC-3' Reverse: 5'-TTCCTTCTCGCACACCAGTT-3'	IDT	N/A
Recombinant DNA		
Mouse Cbl-b sequence-verified cDNA	Laboratory of Gu	N/A
Mouse Cbl sequence-verified cDNA	Laboratory of Gu	N/A
Mouse Irf4 sequence-verified cDNA	Laboratory of Gu	N/A
HA-UB expression vector	Dr.Chen	N/A
pCDNA vector	Invitrogen	Cat#V790-20
MIGR1-MSCV retro-expression vector	Addgene	Plasmid#27490
p3xFlag-CMV™ 7 vector	Sigma	Cat#E7533
MSCV I□B-GFP fusion vector	Dr.Huang	N/A
Software and Algorithms		
Prism(6.0-7.0)	Graphpad	
FlowJo(v9-10)	Treeview	
Volocity	PerkinElmer	

CONTACT FOR REAGEND AND RESOURCE SHARING

Further information and requests for resources and reagents should be directed to and will be fulfilled by the Lead Contact, Hua Gu (hua.gu@ircm.qc.ca)

EXPERIMENTAL MODLE AND SUBJECTED DETAILS

Mice

C57BL/6 mice, B6.SJL mice, μMT mice and Rag1$^{-/-}$ mice were from The Jackson Laboratory. Cbl floxed and Cbl-b$^{-/-}$ mice were described previously (Chiang et al., 2000; Naramura et al., 2002). To generate Cbl$^{-/-}$ Cbl-b$^{-/-}$ mice, Cbl floxed/floxed (Cbl$^{fl/fl}$) and Cbl-b$^{-/-}$ mice were crossed to IgCγ1-Cre transgenic mice kindly provided by S. Casola and K. Rajewsky (Casola et al., 2006). Cbl-b^{C373A} mice were described previously (Oksvold et al., 2008). Animal experimentation was done in accordance with the Canadian Council of Animal Care and approved by the Institut de Recherches Cliniques de Montreal (IRCM) Animal Care Committee.

METHOD DETAILS

Plasmids, cell lines and culture

cDNA encoding *Irf4* was PCR amplified and cloned into plasmid p3xFlag-CMV™ 7 expression vector. cDNAs encoding *Cbl* and *Cbl-b* were separately cloned into pCDNA vector. For the construction of Irf4 overexpression vector, cDNA encoding *Irf4* was cloned into MSCV-MIGR-GFP retroviral vector. IκB-GFP fusion protein retrovirus expression vector was kindly provided by Dr. F. Huang. Hemagglutinin (HA)-tagged ubiquitin vector was a gift from Dr. R. Chen. To prepare retrovirus, Phoenix cells were transfected with the appropriate amount of retroviral vector and package plasmids (30 μg) by Calcium precipitation, according to previous publication (Han et al., 2010). For 40LB culture, naïve WT and Cbl$^{-/-}$ Cbl-b$^{-/-}$ B cells were purified from WT (C57BL-6 or C57BL/6 Mb1-Cre tg) and Cbl$^{fl/fl}$ Cbl-b$^{-/-}$ Mb1-Cre tg) mice by a magnetic column (StemCell Technologies), respectively. GC B cells were purified by FACS sorting. Purified B cells were seeded onto irradiated (900

RAD) 40LB cells described previously (Nojima et al., 2011). B cells were cultured at 37°C for five days, trypsinized and replated onto a fresh 40LB plate for two more days before being subjected to FACS analysis.

Immunization and GC B cell purification

To test T-dependent antibody responses and germinal center reaction, 6 to 10 week-old mice were immunized with either 10^9 sheep red blood cells (SRBCs) (Innovative Research) in PBS or NP_{36}-KLH (BioSources) precipitated in alum adjuvant (Imject Alum, ThemoScientific) by i.p. injection. Mice were analyzed at different days after immunization. To examine the expression of Cbls in GC B cells, SRBC immunized mice were sacrificed at day 8 and B cells were enriched by a magnetic column, stained with anti-B220, CD138, GL7, and Fas. GC ($B220^+$ $GL7^{hi}$ Fas^{hi}) B cells were then purified by FACS sorting on a FACS Aria or Moflo. To obtain a large quantity of GC B cells for *in vitro* stimulation and culture, mice were sequentially immunized at day 0 ($1x10^8$ SRBCs) and day 5 ($1x10^9$ SRBCs) by i.v. injection. Immunized mice were sacrificed at day 12, B cells were enriched by a magnetic B cell enrichment column (StemCell) and subsequently sorted as $B220^+$ $CD138^-$ $GL7^+$ cells. Purity of the isolated GC B cells was confirmed by FACS analysis and was shown to be more than 95% pure for cell surface markers $B220^+$ $GL7^{hi}$ Fas^{hi} (**Figure ES2C**).

Flow cytometric analysis

Total splenic cells or splenic B cells were resuspended in FACS buffer (5%BSA in PBS (PH=7.2)) and stained with the corresponding antibodies on ice for 30 min. Cells were washed twice with FACS buffer and then subjected to analysis on a BD Fortessa or Cyan or to cell sorting on a FACS Aria or Moflo. The following antibodies were used for the staining: anti-B220, anti-GL7, anti-CD11c, anti-CD11b, anti-Gr1, anti-F4/80, anti-NK1.1, anti-Irf4, anti-Igλ, anti-TCRβ, anti-CD3ε, anti-CD86, and anti-CD38 (eBioscience); anti-Fas, anti-CD138, anti-Bcl6, anti-CXCR4, anti-IgG1, anti-IgD (BD Pharmingen). High affinity and total NP-binding B cells and plasma cells were

stained with NP_8-PE, NIP_5-PE, and NP_{38}-PE (BioSearch), respectively. Specificity of NIP_5–APC and NP_{38}-PE to NP-specific but not to carrier protein specific BCRs was confirmed using GC B cells from OVA or NP-OVA immunized mice (**Figure ES2D**). To analyze nuclear proteins Bcl6 and Irf4, total splenic cells were first stained for B220, Fas, and GL7, fixed and permeabilized with FOXP3 staining buffer according to the manufacturer's instructions (eBioscience), and then stained with anti-Bcl6 and Irf4. For cell cycle analysis, mice were injected intravenously with 1 mg of BrdU (BD Pharmingen) in DPBS. Cells were then surface stained with corresponding antibodies, and BrdU labeled cells were stained using an anti-BrdU kit according to the manufacturer's protocols (BD Pharmingen).

qPCR and RNA-Seq analysis

To study the gene expression profiling, naïve B cells and GC ($B220^+CD138^-GL7^+Fas^+$) B cells from wildtype and $Cbl^{-/-}$ $Cbl\text{-}b^{-/-}$ mice were purified by FACS sorting. Total RNAs from sorted cells (pooled from three mice) was extracted using an RNEasy Mini Kit (Qiagen), and reversely transcribed into cDNA using a Reverse-Transcription kit (Invitrogen) according to manufacturer's instructions, respectively.

RNA-seq was performed using the Illumina TruSeq Stranded mRNA Kit according to manufacturer's instructions on an Illumina HiSeq 2000 sequencer. Read quality was confirmed using FastQC v0.10.1. Read alignment was performed using TopHat v2.0.10 on the mouse GRCm38/mm10 genome. Differential expression analysis was performed with DESeq2 from the raw alignment counts calculated with featureCounts. Differentially expressed genes were defined as genes with a |logFC(counts)|>2 and counts > 500 in both experiments. Shown are log2 (counts) expression values of 982 downregulated and 51 upregulated genes in $Cbl^{-/-}$ $Cbl\text{-}b^{-/-}$ than in WT GC B cells.

A SYBR Green PCR mix (Thermo Scientific) and gene-specific primers were used for quantitative RT-PCR analysis (20-50 ng cDNA per reaction). All reactions were done

in triplicates with ViiA7-96 Real Time PCR System (Applied Biosystems). Results were analyzed by the change-in-threshold ($2^{-\Delta\Delta CT}$) method, with β-Actin or GAPDH as 'housekeeping' reference genes, respectively.

Immunofluorescence

Spleens were embedded in optimum cutting temperature compound (Sakura) and flash-frozen in liquid nitrogen. Tissue sections were cut on Cryotome (Leica), fixed in ice-cold acetone (Sigma), blocked with PBS+5%BSA for 1 hour at 25°C, and stained with anti-Cbl (Santa Cruz), anti-Cbl-b (Santa Cruz), anti-CD35 (BD Pharmingen), anti-B220 (BD Pharmingen), and/or PNA (VectorLab), in different combination. The following secondary antibodies were used to detect primary antibodies: anti-Rabbit Alexa-568 (Invitrogen), Streptavidin Alexa-488 (Invitrogen), Streptavidin Alex-633 (Invitrogen). Images were acquired on a Zeiss LSM700 or 710 confocal microscope.

For intracellular staining of Irf4, GC B cell or stimulated GC B cells were purified by FACS sorting. Cells were fixed with 4% PFA, permeabilized with 0.1% Triton X-100, blocked with PBS+5% BSA, and stained with anti-Irf4 (Santa Cruz), followed by anti-Goat Alexa 568 secondary antibody. Cell nucleus was counter stained with DAPI. Images were acquired on a Zeiss LSM710 confocal microscope.

Ig V_H 186.2 gene isolation and DNA sequencing

GC ($B220^+$ Fas^{hi} $GL7^{hi}$ $Ig\lambda^+$ or $B220^+$ Fas^{hi} $GL7^{hi}$ NP38-PE^+) B cells were isolated by FACS from three NP_{36}-KLH immunized WT and $Cbl^{-/-}$ Cbl-$b^{-/-}$ mice, respectively, at day 14 after immunization. Genomic DNA was extracted from the sorted cells using a QuickExtract^{Tm} DNA Extraction Solution (Epicentre). For V_H186.2 sequencing, V_H186.2-J_H2 joints were amplified from genomic DNA by PCR using specific primers for the 5' end of V_H186.2 gene and 3' end of J_H2 gene according to a previous protocol (Dominguez-Sola et al., 2012). PCR products were gel extracted and cloned into a TOPO vector (Invitrogen). High quality traces were analyzed using MacVector

for base pair mismatches and deletions as compared to the germline V_H186.2 gene sequence. Only mismatches mutations in the productive V_H186.2-J_H2 joints were counted as mutations. Ig V_H sequences were analyzed using the IMGT/V-QUEST system to identify the W33L mutation. Primers used were: V_H 186.2: 5'-AGCTGTATCATGCTCTTCTTGGCA -3'; J_H2: 5'-AGATGGAGGCCAGTG AGGGAC -3'.

Enzyme-linked immunospot (ELISPOT) assay and enzyme-linked immunosorbent assay (ELISA)

Total splenic or bone marrow cells were cultured at 37°C in antigen pre-coated 96-well Multiscreen-HA filter plates (Millipore) overnight. Spots of antibody secreting cells were stained with rabbit anti-mouse IgM or IgG1 antibodies conjugated to horseradish peroxidase (Invitrogen), and then developed by addition of AEC substrate (BD Pharmingen). Plates were washed extensively and spots were counted on a dissect microscopy. The antigens used for plate coating were NP_4-OVA and NP_{30}-OVA, respectively. Anti-NP ELISAs were performed as described previously (Jang et al., 2011).

Immunoprecipitation and Immunoblot analysis.

Cells were lysed in TNE buffer (50mM Trise; 140mM NaCl; 5mM EDTA; 0.5% SDS), and immunoblotting was performed following standard procedures. For immunoprecipitation, proteins were immunoprecipitated by incubation of cell lysate overnight at 4°C with the appropriate antibodies (1□g), followed by precipitate the protein-antibody complexes by incubating with protein G agarose (Invitrogen) for another 1 hour at 4°C. Immunoprecipitates were washed four times with TNE buffer, boiled in 40 μl loading buffer and immunoblotted to a PVDF membrane for Western blot analysis. The following antibodies were used for biochemical study: anti-IgM $F(ab)_2$ (BioSource); anti-CD40 (ENZO); anti-Cbl (SantaCruz); anti-Irf4 (SantaCruz); anti-Lamin B (SantaCruz); anti-BLIMP1 (SantaCruz); anti-HA (SantaCruz); anti-Cbl-b (Cell signaling); anti-β□Actin (abcam); anti-Flag (Sigma). Horseradish-peroxidase-conjugated goat anti-rabbit, goat anti-

mouse or donkey anti-goat antibody was used as a secondary antibody, respectively. Membranes were developed with an enhanced chemiluminescence detection system (GE Healthcare).

A Nuclear extraction kit was used to fractionate nuclear and cytoplasmic proteins according to manufacturer's instructions (Active motif).

Bone marrow and Cbl$^{-/-}$ Cbl-b$^{-/-ERCre}$ B cell chimeric mice

To generated Irf4 over-expression or IκB-GFP expressing bone marrow chimeric mice, retroviral stocks were prepared by transfection of Phoenix cells with MSCV-MIGR1 (empty vector), Irf4-MSCV or MSCV-IκB-GFP retroviral vector together with the packaging vector pCL-Eco by the standard calcium transfection (Han et al., 2010). Viral supernatants were collected 48 h and 72 h after the transfection, respectively. To obtain bone marrow stem cells, donor mice were treated with 5-FU (5 mg/mouse, i.p.). Four days later, bone marrow stem cells were collected and cultured under optimal stem cell culture condition. After two-rounds retroviral spin-infections, bone marrow cells were adaptively transferred into lethally irradiated (10 Gy) Rag1$^{-/-}$ recipient mice. Six weeks later, mice were subjected to different immunization regimens.

To generate Cbl$^{-/-}$ Cbl-b$^{-/-ERCre}$ chimeric mice, 1.5x10^{7} splenic B cells from either Cbl-b$^{-/-}$ ER-Cre tg (control) or Cbl$^{fl/fl}$ Cbl-b$^{-/-}$ ER-Cre tg (Cbl$^{-/-}$ Cbl-b$^{-/-ERCre}$) mice were transferred into μMT mice by i. v. injection. Chimeric mice were immunized i.p. with NP-KLH in Alumjet adjuvant the next day (day 0), and given daily tamoxifen (200μg/g body weight) from day 7-10 by oral administration. Mice were sacrificed at day 12, and splenic cells were subjected for FACS analysis. High affinity NP (NIP$_5$-binding) GC B cells and PCs were identified by cell surface and intracellularly staining, respectively, using NIP$_5$-PE in combination with surface markers for GC B cells (B220^{+} GL7^{hi} Fas^{hi}) or PCs (B220$^{-/lo}$ CD138^{+}Lin^{-}).

Cell division and differentiation assay

Purified B cells were labeled with CellTrace fluorescent according to manufacturer's instructions. Cells were cultured on 40LB feeder for five days and then labeled with CellTrace fluorescent according to manufacturer's instructions. Naïve $Cbl^{-/-}$ $Cbl\text{-}b^{-/-}$ B cells were isolated from $Cbl^{fl/fl}$ $Cbl\text{-}b^{-/-}$ Mb1-Cre tg mice. Labeled cells were plated on a fresh 40LB plate and cultured for two more days. Cultured B cells were harvested and cell proliferation was analyzed on a FACS. To examine culture B cell differentiation to PCs, cells were stained with B220, CD138, and Irf4. Irf4 and CD138 positive cells in each cell division were analyzed on a FACS.

STATISTICAL ANALYSIS

Statistical analyses were performed with a two-tailed, unpaired Student's t-test or Fisher's exact t test, with GraphPad Prism V7 software. A *P* value <0.05 was considered statistically significant.

FIGURE LEGENDS

Figure 1. Differential Expression of Cbl and Cbl-b in GC DZ and LZ B Cells

(A) qPCR analysis of *Cbl* and *Cbl-b* mRNA expression in WT naïve and GC B cells. Results were normalized to actin. Expression in naïve B cells was arbitrarily defined as 1. Data reflect mean ± SEM of three independent experiments. $p<0.05$ (unpaired Student's t tests).

(B) Western blot analysis of Cbl and Cbl-b expression in WT none-GC B and GC B cells. Shown are the results of one representative experiment out of two.

(C) Immunofluorescent staining of Cbl and Cbl-b in GC DZ and LZ. GC B cells and the LZ were stained by PNA (green) and anti-CD35 (blue), respectively. Cbl and Cbl-b were visualized in red (Scale bar, 35μm). Shown are the results of one representative out of five individual GCs.

(D) Western blot analysis of Cbl and Cbl-b expression in DZ and LZ GC B cells. DZ and LZ GC B cells were purified by FACS as $B220^{+}GL7^{hi}Fas^{hi}CXCR4^{hi}CD86^{lo}$ and $B220^{+}GL7^{hi}Fas^{hi}CXCR4^{lo}CD86^{hi}$ B cells, respectively. Shown are the results of one representative experiment out of two.

Figure 2. Impaired Antibody Affinity Maturation in $Cbl^{-/-}$ $Cbl\text{-}b^{-/-}$ Mice

(A) Kinetics of serum total anti-NP_{30} antibody titers of IgM and IgG1 isotypes.

(B) The kinetics of serum high affinity anti-NP_4 antibody titers of IgM and IgG1 isotypes.

(C) Antibody affinity maturation of IgG1 antibody. The maturation index is defined by the ratios of anti-NP_4 vs anti-NP_{30} antibody titers.

(D) ELISPOT analysis of splenic ASCs against NP_{30} or NP_4-BSA antigen at day 14 after immunization.

(E) Developmental kinetics of GC B cells in WT and $Cbl^{-/-}$ $Cbl\text{-}b^{-/-}$ mice after NP-KLH immunization. Shown are contour maps (top panel) of GC B cells at day 8 and the statistics (bottom bars) of GC B cell numbers postimmunization.

(F) Analysis of apoptotic GC B cells. Apoptotic GC B cells were visualized by anti-active form Casp staining. Shown are contour plots (left panel) and statistical (right bars) of $Casp^{+}$ GC B cells among total $B220^{+}GL7^{hi}Fas^{hi}$ B cells.

(G) Defective development of high affinity BCR expressing GC B cells in $Cbl^{-/-}$ $Cbl\text{-}b^{-/-}$ mice. Shown at the top panel are the gating strategy for splenic $B220^{+}NP_8$-binding B cells and $IgG1^{+}CD38^{-}$ GC B cells among the gated $B220^{+}NP8^{+}$ cells. Bottom: Statistics of high affinity (NP_8-binding) IgG1 GC B cells in WT and $Cbl^{-/-}$ $Cbl\text{-}b^{-/-}$ mice.

Data are mean± SEM (A-G) and are representative of two or three independent experiments with at least four mice per group. * $p<0.05$; ** $p<0.001$; *** $p<0.0001$ (unpaired Student's t test).

Figure 3. Impaired Selection of High Affinity BCRs but not SHM in $Cbl^{-/-}$ $Cbl\text{-}b^{-/-}$ Mice

(A) Pie presentation of the frequency of SHM in V_H186.2 genes. V_H186.2 genes with different numbers of SHM are shown in different degrees of shade (right). The total numbers of V_H genes analyzed are indicated in the centers of the pies.

(B) Frequency of replacement vs silent mutations in V_H186.2 genes. Each dot represents data from one individual V_H186.2 gene.

(C) Representation of V_H186.2 clones with W33L mutation. The number of W33L clones among VH186.2 sequences is shown in the center of pie chart and was compared using Fisher's exact test. **p<0.001. Data are from pooled five mice each group.

(D) Ratios of replacement vs silent (R/S) mutations in V_H186.2 coding genes.

(E) Development of NIP_5 and NP_{38}-binding GC B cells at different time points of GC reaction. Shown (top panel) are flow cytometric analyses of splenic NP_{38} or NIP_5-binding cells in gated 220^+ $GL7^{hi}$ Fas^{hi} GC B cells at day 8 and day 14 post NP-KLH immunized. Bottom left and middle: statistics of NP_{38} and NIP_5-binding GC B cells at day 8 and 14 after immunization, respectively. Bottom right: Percentages of high affinity NP (NIP_5-binding) GC B cells among total NP specific (NP_{38}-binding) GC B cells at day 8 and day 14 after immunization. Data are mean± SEM (E) and are representative of two independent experiments with five mice per group. ** p<0.001; *** p<0.0001 (unpaired Student's t test).

Figure 4. Expedited PC Differentiation of High Affinity GC B Cells in the Absence of Cbls

(A) *In vivo* newly generated PCs identified by BrdU labeling assay. Shown are flow cytometric (left) and statistics analyses (right) of splenic newly generated PCs after 24 hours BrdU labeling, identified as $Lin^-BrdU^+CD138^+$ cells.

(B) The *in vivo* rates of PC genesis presented as the total numbers of newly generated PCs either per spleen (left) or per hour in the spleen (right).

(C) Flow cytometric analyses of total (top panel), and NIP_5-binding (bottom panel) GC B cells at day 12 without (left) or with ER-Cre mediated Cbl ablation (right). Statistics (right) are shown as bars.

(D) *In vitro* PC differentiation of naïve WT and Cbl$^{-/-}$ Cbl-b$^{-/-}$ B cells from Cbl$^{fl/fl}$ Cbl-b$^{-/-}$ Mb1-Cre tg mice in 40LB feeder cell culture. Shown are flow cytometric (left) and statistical (right) analyses of (CD138^{+}B220$^{hi/lo}$) PCs/plasma blast-like cells.

(E) Comparison of *In vitro* differentiation of freshly isolated WT and Cbl$^{-/-}$ Cbl-b$^{-/-}$ (Lin^{-}B220^{+} GL7^{hi}) GC B cells. Purities of the isolated GC B cells are shown in Figure S9B). Shown are flow cytometric (left) and statistical (right) analyses of plasma blast-like (B220^{+}CD138^{hi}) cells generated in the culture.

(F) Cell division dependent B-cell differentiation to PCs in 40LB feeder culture system. Shown are dot plots (left) and histogram analyses (right) of Irf4 expression in cell divisions 1st, 2nd, 3rd, and 4th WT or Cbl$^{-/-}$ Cbl-b$^{-/-}$ B cells (Cbl$^{fl/fl}$ Cbl-b$^{-/-}$ Mb1-Cre tg) identified by Cell Trace dilution.

Data are mean± SEM (A-F) and are representative of two or three independent experiments with at least four mice per group. * $p<0.05$; ** $p<0.001$ (unpaired Student's t test).

Figure 5. Post-Transcriptional Regulation of GC Differentiation Program by Cbls

(A) qPCR analysis of GC B cell and PC identity genes in WT and Cbl$^{-/-}$ Cbl-b$^{-/-}$ GC B cells. Data were from FACS purified splenic B220^{+} GL7^{hi} Fas^{hi} GC B cells pooled from 3x WT and Cbl$^{-/-}$ Cbl-b$^{-/-}$ mice at day 8 after SRBC immunization.

(B) Comparison of the expression of protein synthesis and secretion related genes which are upregulated in PCs in WT and Cbl$^{-/-}$ Cbl-b$^{-/-}$ GC B cells based on RNA-seq. Shown are the folds of increased expression in Cbl$^{-/-}$ Cbl-b$^{-/-}$ relative to WT GC B cells

(C) Western blot analysis of Irf4 in WT and Cbl$^{-/-}$ Cbl-b$^{-/-}$ B220^{+} GL7^{hi} CD138^{-} GC B cells GC B cells.

(D and E) Flow cytometric analyses of Irf4 vs Bcl6 expression in GC B cells without (D) or with (E) anti-CD40 and BCR stimulation. Shown are contour maps (top panel) and statistics (bottom panel) of Irf4^{hi} Bcl6^{lo} and Bcl6^{hi} cells among total gated B220^{+} GL7^{hi} Fas^{hi} GC B cells.

(F) Western blot analysis of Irf4 expression in WT and Cbl$^{-/-}$ Cbl-b$^{-/-}$ B220^{+}GL7^{hi} CD138^{-} GC B cells with or without anti-CD40 and BCR stimulation.

Data are mean ± SEM (A, D, E) and are representative of two or three independent experiments (A, C, D, E, F) with at least four mice per group. ** $p<0.001$; *** $p<0.0001$ (unpaired Student's t test).

Figure 6. Regulation of Nuclear Irf4 Ubiquitination and Expression by Cbls

(A and B) Confocal microscopic analysis of cytosolic and nuclear Irf4 in WT and Cbl$^{-/-}$ Cbl-b$^{-/-}$ GC B cells without (A) or with (B) anti-CD40 and BCR stimulation. The statistical analyses show the percentages of nucleus vs total IRrf4. Each dot represents one cell.

(C) Western blot analysis of nuclear vs cytosolic Irf4 in WT and Cbl$^{-/-}$ Cbl-b$^{-/-}$ B220^{+} GL7^{hi} CD138^{-} GC B cells before and after anti-CD40 and BCR stimulation.

(D) Asymmetric expression of Cbl and Cbl-b vs Irf4 proteins in WT B220^{+} GL7^{hi} CD138^{-} GC B cells before and after CD40 and BCR stimulation.

(E) Co-immunoprecipitation and Western blot analysis of Cbl and Cbl-b association with Flag tagged Irf4 (Irf4-Flag).

(F) Irf4 ubiquitination by Cbl or Cbl-b. Shown are Western blot analyses of ubiquitinated Irf4-Flag immunoprecipitated from 239T cells cotransfected with either Cbl or Cbl-b.

(G) Association of Irf4 with Cbl or Cbl-b in freshly isolated WT GC B cells.

(H) Ubiquitination of Irf4 in WT and Cbl$^{-/-}$ Cbl-b$^{-/-}$ *in vitro* generated GC (iGC) B cells.

Data are mean± SEM (A-B) and are representative of two independent experiments (A-G). ** $p<0.001$; *** $p<0.0001$ (unpaired Student's t test).

Figure 7. Impaired Development of High Affinity GC B Cells in Cbl$^{-/-}$ Cbl-b$^{-/C373A}$ or MSCV-Irf4 BM Chimeric Mice

(A-C) Impaired GC affinity maturation in Cbl$^{-/-}$ Cbl-b$^{-/C373A}$ mice as compared to WT and Cbl$^{-/-}$ Cbl-b$^{-/+}$ IgCγ-Cre tg controls (day 12 after NP-KLH immunization). (A) Dot plots (left) and statistical (right) analyses of Fas^{+} GL7^{+} GC B cells among gated

splenic $B220^+$ cells. (B) Flow cytometric (left) and statistical (right) analyses of high affinity (NP_8-binding) GC B cells among total $B220^+$ cells. Shown are the gating strategy of splenic $B220^+NP_8$-binding B cells (top left panel), high affinity NP specific $IgG1^+CD38^-$ GC B cells (bottom left panel), and statistics of high affinity NP binding GC B cells. (C) The statistics of splenic total (anti-NP_{30}-binding antibody) and high affinity (NP_4–binding antibody) secreting plasma cells (ASCs).

(D-F) Ectopic expression of Irf4 abolishes high affinity antibody producing GC B cell development in MSCV-Irf4 BM chimeric mice after NP-KLH immunization (day 12). WT BM stem cells were transduced with either MIGR-MSCV-GFP (empty) or MSCV-GFP-Irf4 retroviral vector and used to generate BM chimeras. (D) Dot plots (left) and statistical (right) analyses of Fas vs GL7 staining of gated $B220^+$ $IgD^{-/lo}$ splenic GC B cells. (E) Contour plots (top) and statistical (bottom) analyses of splenic high affinity (NP_8-binding) $IgG1^+CD38^-$ GC B cells in BM chimeras with (GFP^+) without (GFP^-) retrovirus infection. (F) Histogram analysis of $B220^-CD138^+$ splenic PCs among GFP^+ $Linage^-$ splenocytes in empty MIGR-MSCV and Irf4-MSCV infected BM chimeras.

Data are mean ± SEM (A-F) and are representative of two or three independent experiments with at least five mice per group. * $p<0.05$; ** $p<0.001$ (unpaired Student's t test).

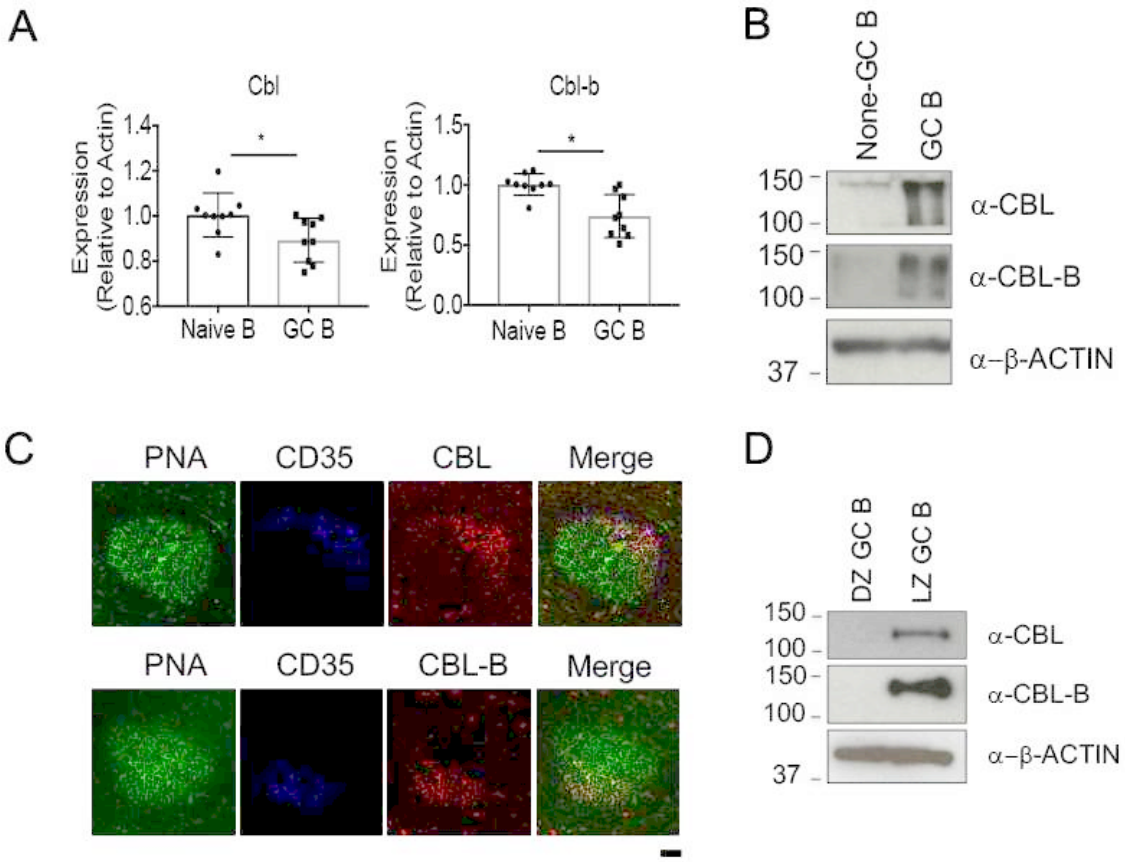
A
Cbl
Expression (Relative to Actin)
1.4
1.2
1.0
0.8
0.6
*
Naive B
GC B
Cbl-b
Expression (Relative to Actin)
1.5
1.0
0.5
0.0
*
Naive B
GC B
B
None-GC B
GC B
150
100
150
100
37
α-CBL
α-CBL-B
α–β-ACTIN
C
PNA
CD35
CBL
Merge
PNA
CD35
CBL-B
Merge
D
DZ GC B
LZ GC B
150
100
150
100
37
α-CBL
α-CBL-B
α–β-ACTIN

Figure 1

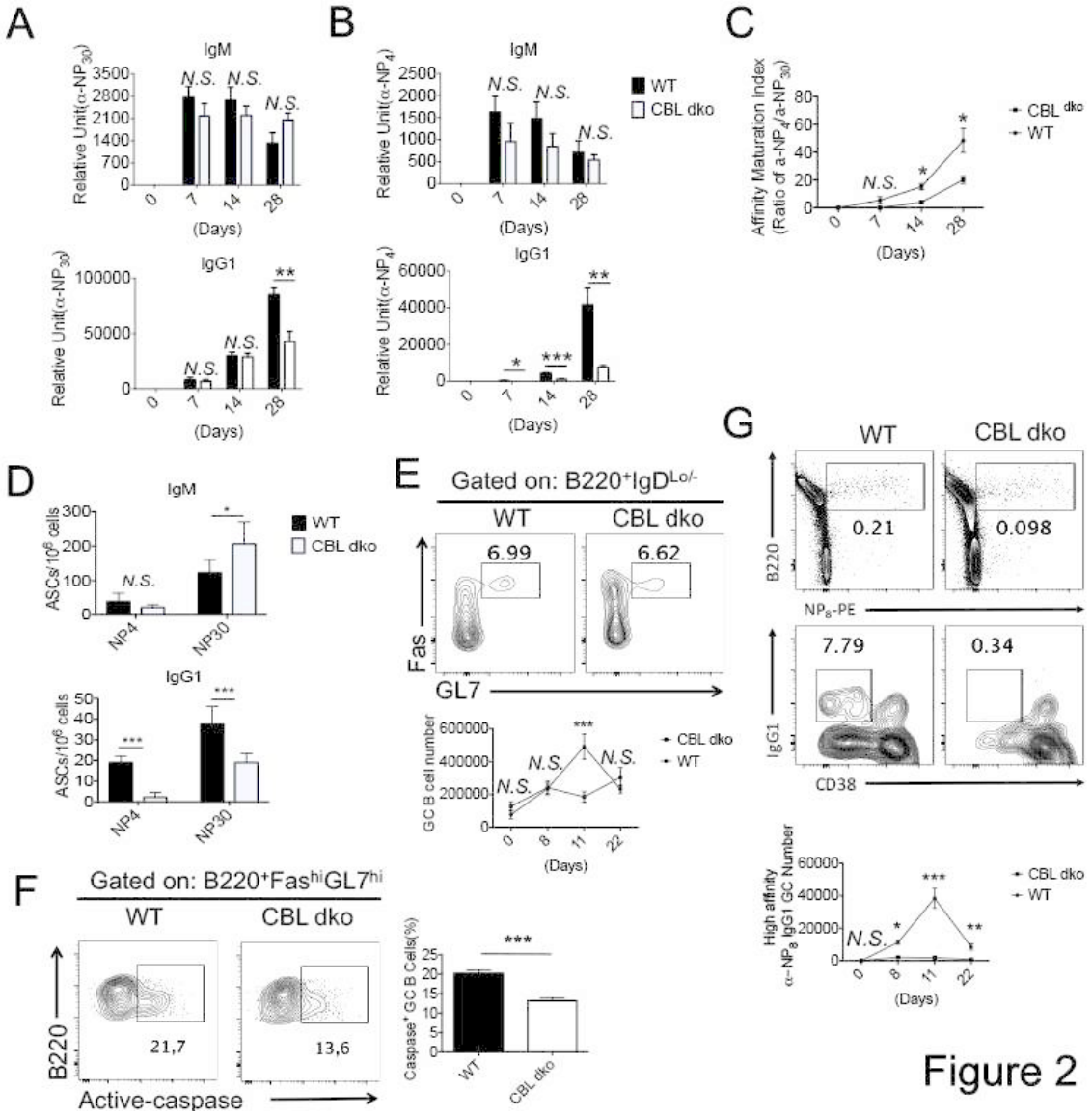
A
IgM
Relative Unit(α-NP30)
N.S.
(Days)
IgG1
B
IgM
Relative Unit(α-NP4)
WT
CBL dko
IgG1
C
Affinity Maturation Index
(Ratio of a-NP4/a-NP30)
CBL dko
WT
D
IgM
ASCs/10^6 cells
NP4
NP30
IgG1
E
Gated on: B220+IgDLo/-
WT
CBL dko
6.99
6.62
Fas
GL7
GC B cell number
F
Gated on: B220+FashiGL7hi
21,7
13,6
B220
Active-caspase
Caspase+ GC B Cells(%)
G
0.21
0.098
NP8-PE
7.79
0.34
IgG1
CD38
High affinity
α-NP8 IgG1 GC Number

Figure 2

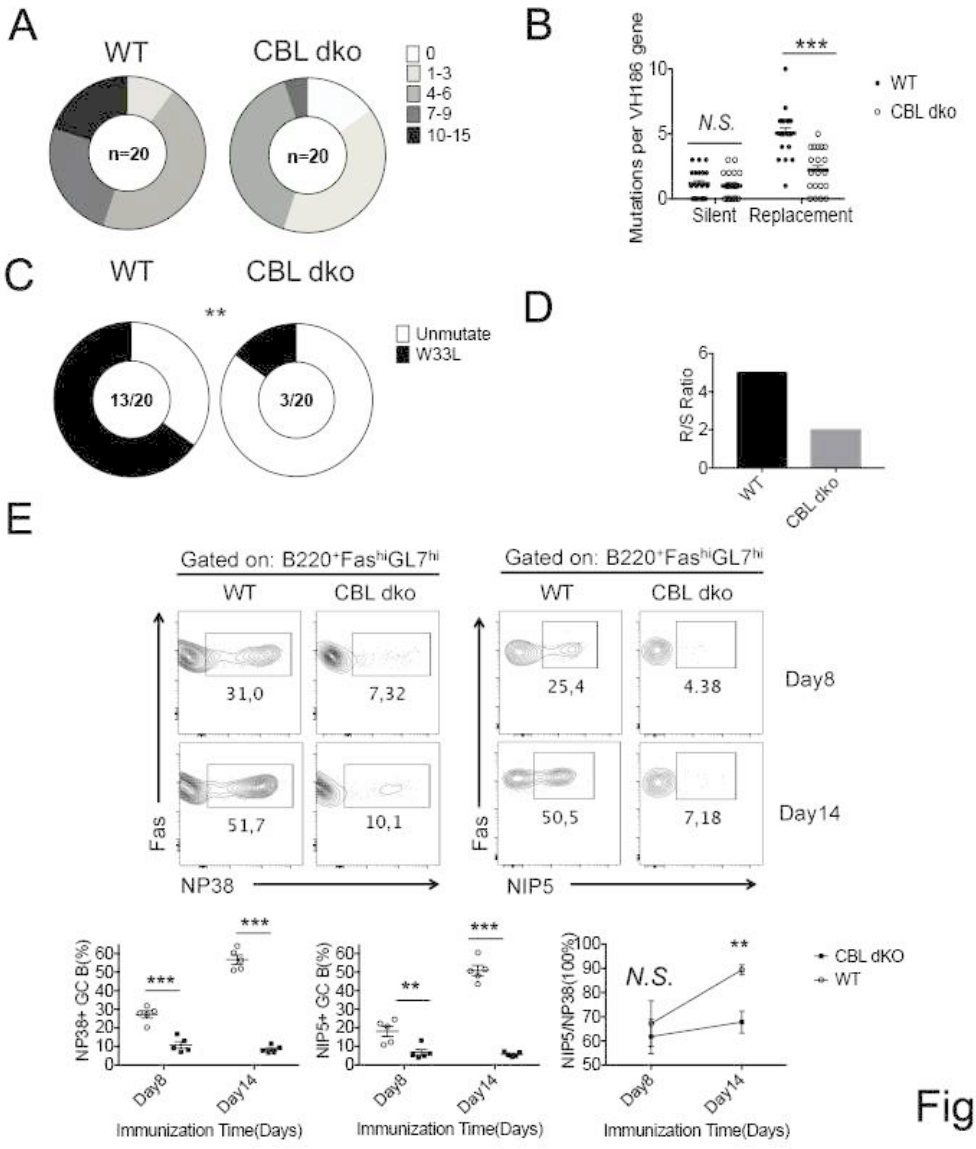
A
WT
CBL dko
0
1-3
4-6
7-9
10-15
n=20
n=20
B
Mutations per VH186 gene
***
N.S.
WT
CBL dko
Silent
Replacement
C
WT
CBL dko
**
Unmutate
W33L
13/20
3/20
D
R/S Ratio
WT
CBL dko
E
Gated on: B220+FashiGL7hi
Gated on: B220+FashiGL7hi
WT
CBL dko
WT
CBL dko
31,0
7,32
25,4
4.38
Day8
51,7
10,1
50,5
7,18
Day14
Fas
NP38
Fas
NIP5
NP38+ GC B(%)
NIP5+ GC Bi(%)
NIP5/NP38(100%)
N.S.
CBL dKO
WT
Day8
Day14
Immunization Time(Days)
Immunization Time(Days)
Immunization Time(Days)

Figure 3

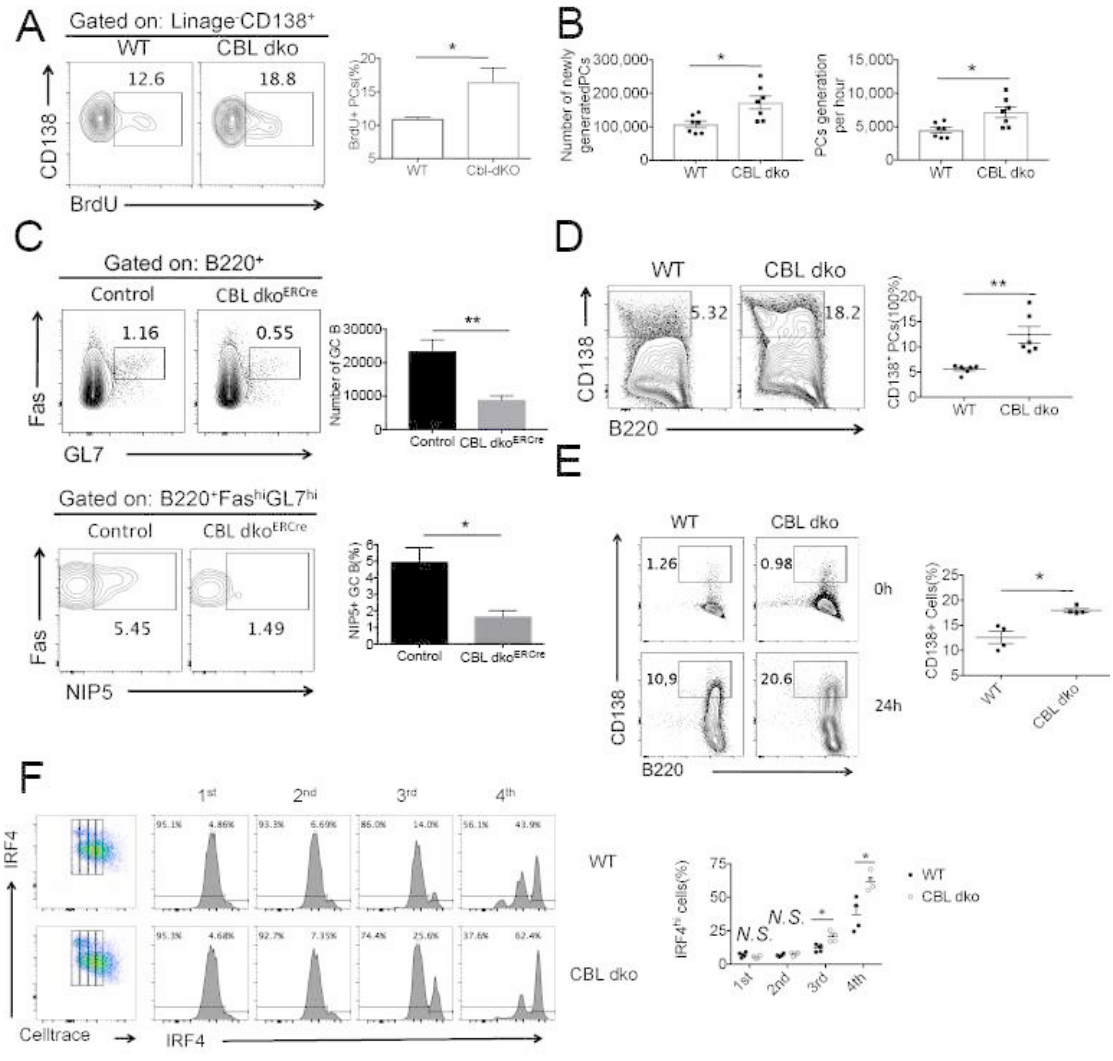
A
Gated on: Linage-CD138+
WT
CBL dko
12.6
18.8
CD138
BrdU
BrdU+ PCs(%)
WT
Cbl-dKO
B
Number of newly generated PCs
PCs generation per hour
WT
CBL dko
C
Gated on: B220+
Control
CBL dkoERCre
1.16
0.55
Fas
GL7
Number of GC B
Gated on: B220+FashiGL7hi
5.45
1.49
NIP5
NIP5+ GC B(%)
D
5.32
18.2
CD138+ PCs(100%)
E
1.26
0.98
10,9
20.6
0h
24h
CD138+ Cells(%)
F
1st
2nd
3rd
4th
IRF4
Celltrace
WT
CBL dko
IRF4hi cells(%)
N.S.

Figure 4

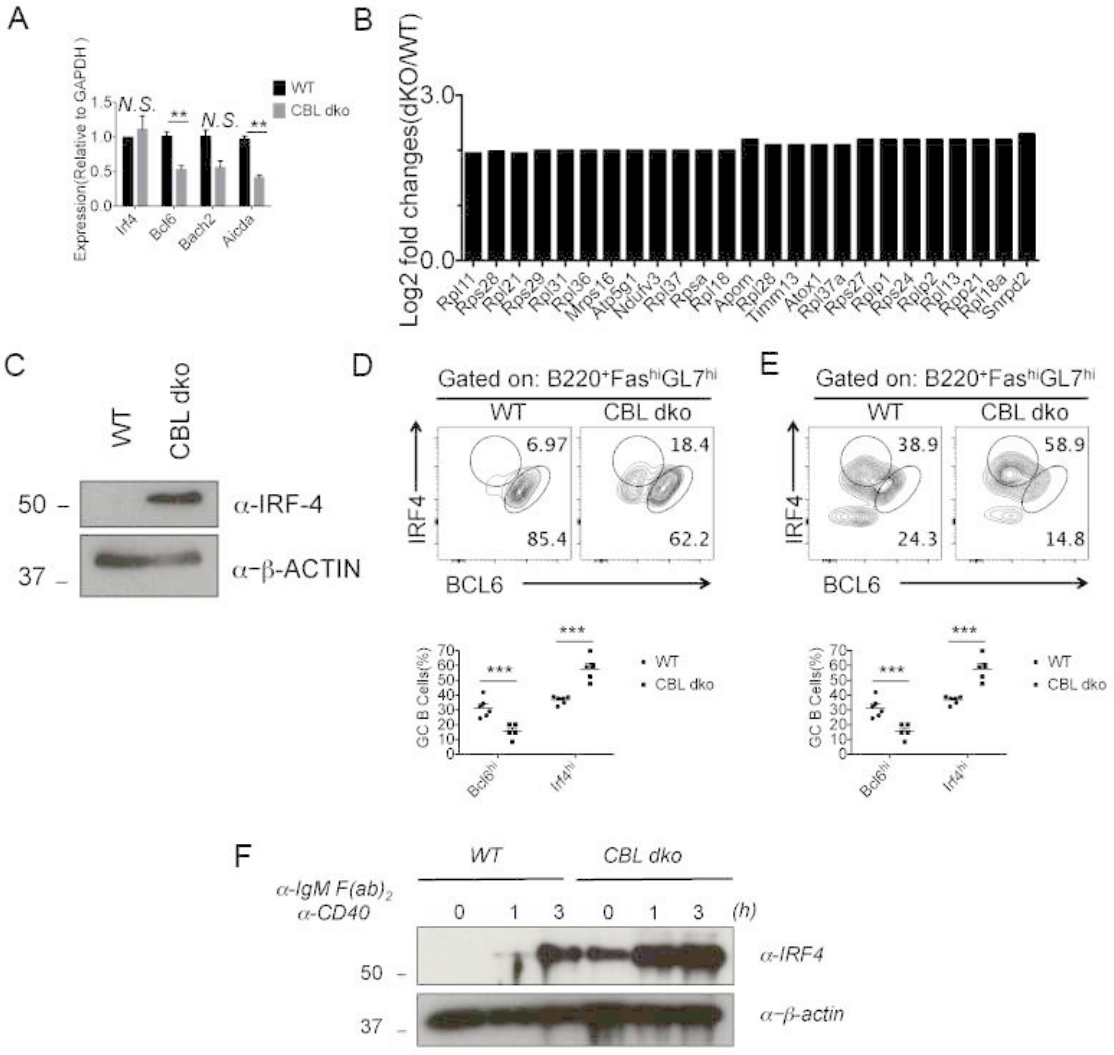
A
Expression(Relative to GAPDH)
WT
CBL dko
N.S.
**
N.S.
**
Irf4
Bcl6
Bach2
Aicda
B
Log2 fold changes(dKO/WT)
3.0
0.0
Rpl11
Rps28
Rpl21
Rps29
Rpl31
Rpl36
Mrps16
Atp5g1
Ndufv3
Rpl37
Rpsa
Rpl18
Apom
Rpl28
Timm13
Atox1
Rpl37a
Rps27
Rplp1
Rps24
Rplp2
Rpl13
Rpp21
Rpl18a
Snrpd2
C
WT
CBL dko
50
37
α-IRF-4
α-β-ACTIN
D
Gated on: B220+FashiGL7hi
WT
CBL dko
6.97
18.4
85.4
62.2
IRF4
BCL6
GC B Cells(%)
***
***
WT
CBL dko
Bcl6hi
Irf4hi
E
Gated on: B220+FashiGL7hi
WT
CBL dko
38.9
58.9
24.3
14.8
IRF4
BCL6
GC B Cells(%)
***
***
WT
CBL dko
Bcl6hi
Irf4hi
F
WT
CBL dko
α-IgM F(ab)2
α-CD40
0 1 3 0 1 3 (h)
50
37
α-IRF4
α-β-actin

Fiugre 5

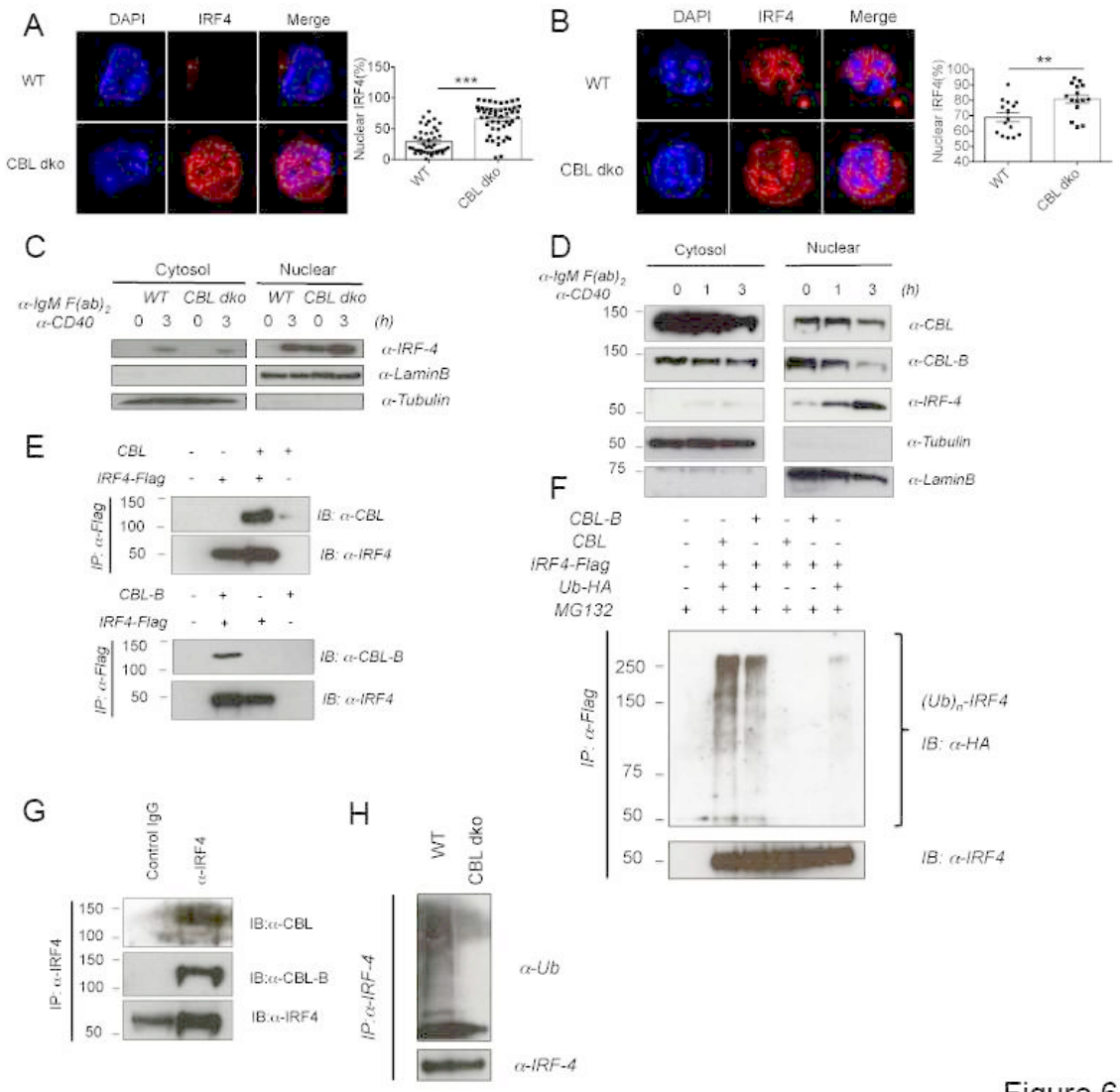
A
DAPI
IRF4
Merge
WT
CBL dko
Nuclear IRF4(%)
***
B
**
C
Cytosol
Nuclear
α-IgM F(ab)2
α-CD40
WT CBL dko WT CBL dko
0 3 0 3 0 3 0 3 (h)
α-IRF-4
α-LaminB
α-Tubulin
D
0 1 3 0 1 3 (h)
α-CBL
α-CBL-B
α-IRF-4
α-Tubulin
α-LaminB
E
CBL
IRF4-Flag
IP: α-Flag
IB: α-CBL
IB: α-IRF4
CBL-B
IB: α-CBL-B
F
CBL-B
CBL
IRF4-Flag
Ub-HA
MG132
IP: α-Flag
(Ub)n-IRF4
IB: α-HA
IB: α-IRF4
G
Control IgG
α-IRF4
IP: α-IRF4
IB:α-CBL
IB:α-CBL-B
IB:α-IRF4
H
WT
CBL dko
IP: α-IRF-4
α-Ub
α-IRF-4

Figure 6

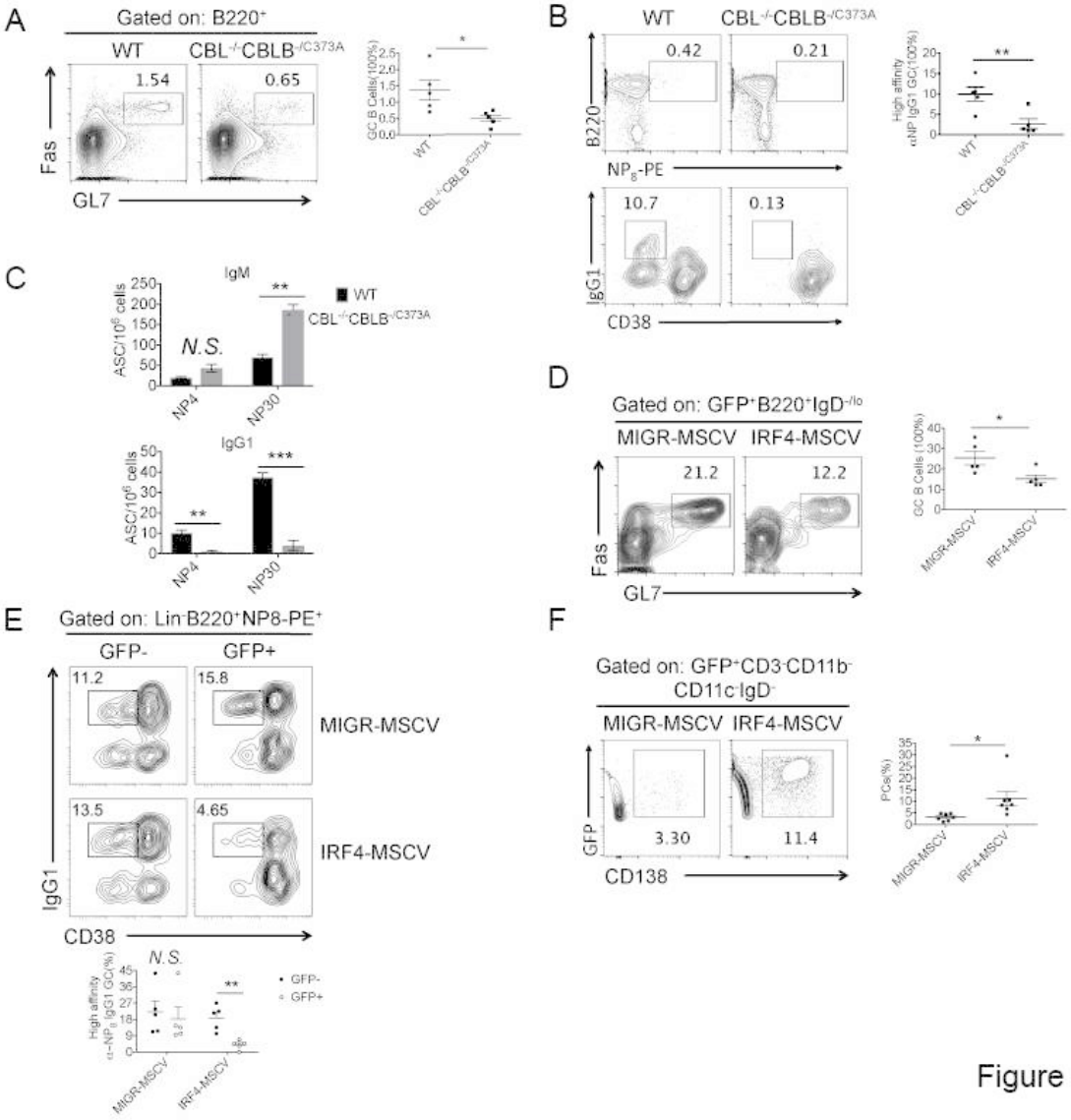
A
Gated on: B220+
WT
CBL-/-CBLB-/C373A
1.54
0.65
Fas
GL7
GC B Cells (100%)
WT
CBL-/-CBLB-/C373A
B
WT
CBL-/-CBLB-/C373A
0.42
0.21
B220
NP8-PE
10.7
0.13
IgG1
CD38
High affinity α-NP IgG1 GC(100%)
C
IgM
WT
CBL-/-CBLB-/C373A
ASC/10^6 cells
N.S.
NP4
NP30
IgG1
D
Gated on: GFP+B220+IgD-/lo
MIGR-MSCV
IRF4-MSCV
21.2
12.2
Fas
GL7
GC B Cells (100%)
E
Gated on: Lin-B220+NP8-PE+
GFP-
GFP+
11.2
15.8
MIGR-MSCV
13.5
4.65
IRF4-MSCV
IgG1
CD38
N.S.
High affinity α-NP8 IgG1 GC(%)
GFP-
GFP+
F
Gated on: GFP+CD3-CD11b-
CD11c-IgD-
MIGR-MSCV
IRF4-MSCV
3.30
11.4
GFP
CD138
PCs(%)

Figure 7